NEA/NSC/DOC(98)7
INDC(Ger)-044
Jül-3550

PROGRESS REPORT ON NUCLEAR DATA RESEARCH IN THE FEDERAL REPUBLIC OF GERMANY

for the Period April 1, 1997 to March 31, 1998

June 1998

Edited by
S. M. Qaim
Forschungszentrum Jülich GmbH
Institut für Nuklearchemie
Jülich, Federal Republic of Germany

NEA/NSC/DOC(98)7
INDC(Ger)-044

Jül-3550
Berichte des Forschungszentrums Jülich; 3550

Edited by: S.M. Qaim
Forschungszentrum Jülich GmbH
Institut für Nuklearchemie
Jülich, Federal Republic of Germany

FOREWORD

As in previous years, this report has been prepared to promote the exchange of nuclear data research information between the Federal Republic of Germany and other member states of OECD/NEA and IAEA. It covers progress reports from the research centres at Karlsruhe and Jülich, the universities of Dresden, Hannover, Köln, Mainz, Marburg, München as well as from the PTB Braunschweig. The emphasis in the work reported here is on measurement, compilation and evaluation of nuclear data for pure and applied science programmes, such as those relevant to fission- and fusion-reactor technology, accelerator shielding and development, astrophysics research, cosmogenic and meteoritic investigations, radiation therapy, production of medically important radioisotopes, etc.

The coordination of nuclear data activities at the international level is done by two committees: the NEA-Nuclear Science Committee (NEA-NSC) and the IAEA-International Nuclear Data Committee (INDC). The present Editor has the privilege and the responsibility of representing Germany in both the committees. This report should therefore also serve as a background information to some areas of work of those committees.

Each contribution is presented under the laboratory heading from where the work is reported. The names of other participating laboratories are also mentioned. When the work is relevant to the World Request List for Nuclear Data, WRENDA 93/94 (INDC(SEC)-104/U+G), the corresponding identification numbers are given.

Jülich, June 1998 S.M. Qaim

This document contains information of a preliminary nature. Its contents should be used with discretion.

CONTENTS

Forschungszentrum Karlsruhe
Institut für Kernphysik

1. The (n,γ) Cross Section of ^{7}Li*

M. Heil, F. Käppeler, M. Wiescher[1], and A. Mengoni [2]

The nucleosynthesis regime of the standard Big Bang is restricted to the isotopes of H, He, and Li due to the instability gaps at A=5 and A=8. In view of small but significant abundances of nuclei with A>8 even in the oldest stars, the discussion of inhomogeneous big bang scenarios offered a possibility to bridge the instability gaps in the related neutron rich, low-density zones. A main reaction sequence in these scenarios is ^{7}Li(n,γ)^{8}Li(α,n)^{11}B(n,γ)^{12}B($\beta^{-}\nu$)^{12}C.
Previous cross section measurements of the important ^{7}Li(n,γ)^{8}Li reaction show large discrepancies. The present experiment was carried out with an improved technique that allowed to eliminate a number of systematic uncertainties. A thin sample of natural LiF on a supported carbon backing was mounted in a double grid ionization chamber. Repeated irradiations for ~2 sec in a well defined neutron beam were monitored via the ^{6}Li(n,α) reaction, while the induced ^{8}Li activity was measured between the irradiations via the 2α-decay of ^{8}Be. The overall sensitivity could be greatly enhanced by the coincident observation of the reaction and decay products in the two modes of the experiment. The cross section was measured at neutron energies of E_n=5 meV and E_n=54 keV. With the present results and the reanalysis of a previous measurement the discrepancy among existing data could be resolved and the cross section be determined with improved accuracy.

*in *Nuclear Data for Science and Technology*, edited by G. Reffo, A. Ventura, and C. Grandi, (Italian Physical Society, Bologna, 1997), p. 1618.

2. The Stellar Neutron Capture Cross Section of ^{34}S*

R. Reifarth, K. Schwarz, F. Käppeler

Neutron capture nucleosynthesis in massive stars is known to produce most of the *s*-process yields between Fe and Sr, but contributes also significantly to the observed abundances of some lighter isotopes. In this context, the (n,γ) cross section of ^{34}S is important for the production of ^{36}S which may be interpreted as a monitor for the integrated neutron exposure during the late evolutionary stages of massive stars.
The (n,γ) cross section of ^{34}S has been measured by means of the activation technique using a quasi-stellar neutron spectrum for a thermal energy of kT=25 keV. In a first attempt, a cross section of 0.5±0.1 mb was obtained, significantly smaller than the 2.9 mb predicted theoretically. In view of this discrepancy and in order to reduce the remaining uncertainty, the measurement was repeated with an improved experimental setup. The main achievements in this respect were an optimized sample preparation as well as the complementary use of Si(Li) detectors and PIN-diodes for measuring the induced ^{35}S activity.

*in *Nuclear Data for Science and Technology*, edited by G. Reffo, A. Ventura, and C. Grandi, (Italian Physical Society, Bologna, 1997), p. 1621.

[1]University of Notre Dame, Notre Dame, USA
[2]ENEA, Bologna, Italy

3. Measurement of Direct Neutron Capture by Neutron-Rich Sulfur Isotopes*

H. Beer, C. Coceva[1], R. Hofinger[2], P. Mohr[2], H. Oberhummer[2], P. Sedyshev[3], and Y. Popov[3]

Thermal neutron capture cross sections for ^{34}S and ^{36}S have been measured and spectroscopic factors for the final states have been extracted. The calculated direct–capture cross sections reproduce the experimental data.

*Nucl. Phys. **A621** (1997) 235c.

4. Measurement and Analysis of Neutron Capture Reaction Rates of Light Neutron-Rich Nuclei*

P. Mohr[2], H. Beer, H.Herndl[2], and H. Oberhummer[2]

Several neutron capture cross sections of light neutron-rich nuclei were measured in the astrophysically relevant energy region of 5 to 200 keV. The experimental data are compared to calculations using the direct capture model. The results are used for the calculation of neutron capture cross sections of unstable isotopes. Furthermore, neutron sources with energies below $E_n \approx 10$ keV are discussed.

*in *Nuclear Data for Science and Technology*, edited by G. Reffo, A. Ventura, and C. Grandi, (Italian Physical Society, Bologna, 1997), p. 1596.

5. (p,γ)-Rates of Ruthenium and Molybdenum Isotopes for Explosive Nucleosynthesis Studies*

J. Bork, T. Sauter, F. Käppeler, H. Schatz[4], and T. Rauscher[5]

The origin of the 32 neutron deficient nuclei between ^{74}Se and ^{196}Hg, the so-called *p*-nuclei, is generally attributed to photodisintegration reactions on a neutron-rich seed during supernova explosions. In certain astrophysical scenarios the most abundant p-nuclei ^{92}Mo, ^{94}Mo, ^{96}Ru and ^{98}Ru are notoriously underproduced. Since proton capture reactions may contribute significantly to these nuclei, the respective (p,γ)-rates are an important input for such models. Due to the lack of experimental data in the A $\geq$ 70 region, these rates are yet completely based on theoretical calculations.
As an experimental check, (p,γ) cross section measurements were started at the Karlsruhe Van de Graaff accelerator for a number of molybdenum and ruthenium isotopes. By using the activation technique, the cross sections of several isotopes could be determined simultaneously. The samples, which consisted of thin metallic layers sputtered on aluminum backings, were exposed to typical beam currents of 20 to 50 μA. In most cases, the (p,γ) cross sections could be deduced with uncertainties of less than 5%. In this study, which was performed in the relevant proton energy range from 1.5 to 3 MeV, differences of up to a factor two were obtained between the experimental cross sections and theoretical Hauser-Feshbach predictions.

*in *Nuclear Data for Science and Technology*, edited by G. Reffo, A. Ventura, and C. Grandi, (Italian Physical Society, Bologna, 1997), p. 1593;
Phys. Rev. C **55** (1997) 3127.

[1]ENEA, Bologna, Italy
[2]Technical University, Vienna, Austria
[3]JINR Dubna, Russia
[4]University of Notre Dame, Notre Dame, USA
[5]University of Basel, Basel, Switzerland

6. The Stellar (n,γ) Cross Section of the Unstable Isotope ^{135}Cs*

S. Jaag, F. Käppeler, G. Reffo[1], and P. Koehler[2]

The (n,γ) cross section of the unstable isotope ^{135}Cs has been measured relative to that of gold by means of the activation method. The sample was produced by ion implantation in a high resolution mass separator and irradiated in a quasi-stellar neutron spectrum for $kT = 25$ keV using the ^{7}Li(p,n)^{7}Be reaction near threshold. The $\sim 8\,\%$ uncertainty of the resulting stellar cross sections is dominated by the thermal (n,γ) cross section used for sample definition. The experimental data are complemented by a set of calculated cross sections for the Cs isotopes. The improved cross sections are used for an s-process analysis of the ^{134}Cs-branching.

*_Nucl. Phys._ **A621** (1997) 247c.

7. Gamma-Ray Production Cross Sections from keV Neutron Captures in Barium Isotopes*

F. Voss, K. Wisshak, F. Käppeler

The Karlsruhe 4πBaF$_2$ detector has been used for several years to determine accurate (n,γ) cross sections for neutron capture nucleosynthesis in Red Giant stars. In the course of these studies the detector was operated part time in the spectroscopy mode by analyzing the time and energy signals of all 41 detector modules independently with an ADC system. After correction of the raw data, in particular for cross talking between modules, detector efficiency, and energy resolution, the related capture γ–ray spectra and γ–ray production cross sections can be extracted. This analysis is presented for the barium isotopes 134, 135, 136, and 137 resulting in γ–ray production cross sections in the neutron energy interval between 20 and 200 keV.

*in *Nuclear Data for Science and Technology*, edited by G. Reffo, A. Ventura, and C. Grandi, (Italian Physical Society, Bologna, 1997), p. 607.

8. Stellar Neutron Capture Cross Sections of the Nd Isotopes*

K. Wisshak, F. Voss, F. Käppeler, L. Kazakov[3], and G. Reffo[1]

The neutron capture cross sections of ^{142}Nd, ^{143}Nd, ^{144}Nd, ^{145}Nd, ^{146}Nd, and ^{148}Nd have been measured in the energy range from 3 to 225 keV at the Karlsruhe 3.75 MV Van de Graaff accelerator. Neutrons were produced via the ^{7}Li(p,n)^{7}Be reaction by bombarding metallic Li targets with a pulsed proton beam. Capture events were registered with the Karlsruhe 4π Barium Fluoride Detector. The cross sections were determined relative to the gold standard. The experiment was difficult due to the small cross sections of the even isotopes at or near the magic neutron number N=82, and also since the isotopic enrichment of some samples was comparably low. The necessary corrections for capture of scattered neutrons and for isotopic impurities could be determined reliably thanks to the high efficiency and the spectroscopic quality of the BaF$_2$ detector.
Correspondingly, a consistent set of (n,γ) cross sections for the six stable neodymium isotopes involved in the s process with typical uncertainties of 1.5–2% could be established. From these data, Maxwellian averaged cross sections were calculated between kT = 10 keV and 100 keV. The resulting astrophysical implications were investigated in an s–process analysis based on the classical approach, which deals with the role of the s–only isotope ^{142}Nd for the Nσ–systematics

[1]Centro Dati Nucleari, Bologna, Italy
[2]Oak Ridge National Laboratory, Oak Ridge, USA
[3]Institute for Physics and Power Engineering, Obninsk, Russia

near the magic neutron number N=82, the decomposition of the Nd abundances into the respective $r-$, $s-$, and $p-$process components, and the interpretation of isotopic anomalies in meteoritic material.

* Phys. Rev. C **57** (1998) 391.

9. The Stellar (n,γ) Cross Sections of the Stable Iridium Isotopes*

S. Jaag

The existing keV neutron capture cross section data of the stable Ir isotopes 191 and 193 exhibit large discrepancies and have never been published in their final versions (1,2). Therefore, the stellar cross sections of these isotopes have been remeasured relative to that of gold by means of the activation method. Metallic samples were irradiated in a quasi–stellar neutron spectrum for $kT = 25\,keV$ using the ^{7}Li(p,n)^{7}Be reaction near threshold. The resulting stellar cross sections of ^{191}Ir and ^{193}Ir show uncertainties of 4 and 7 %, respectively, and are in excellent agreement with Ref. (1).

(1) R.L. Macklin, D.M. Drake, and J.J. Malanify,
Report LA-7479-MS, Los Alamos Scientific Laboratory, 1978.
(2) P.E. Koehler and F. Käppeler,
AIP Conference Proceedings 327, Nuclei in the Cosmos III (1994), p. 157.

Nucl. Phys.* **A621 (1997) 251c.

10. Stellar Capture Rates for s–Process Strong ComponentElements*

P. Mutti[1], F. Corvi[1], K. Athanassopulos[1], H. Beer, P. Krupchitsky[2]

Neutron capture resonances in ^{207}Pb and ^{209}Bi have been studied at the GELINA electron linear accelerator in the energy ranges 0.2 – 200 and 0.2 – 80 keV, respectively. Maxwellian average cross sections were calculated from the measured capture areas for thermal energies from 5 to 50 keV. These data were used in a parameterized model to determine the abundance contributions from the main and strong s–process components. In combination with calculated r–process abundances it was possible to reproduce the solar abundance pattern in the mass region 204<A<209 and to confirm that ^{209}Bi is predominantly of r–process origin.

*in *Nuclear Data for Science and Technology*, edited by G. Reffo, A. Ventura, and C. Grandi, (Italian Physical Society, Bologna, 1997), p. 1584.

[1]JRC, IRMM, Geel, Belgium
[2]Institute of Thoretical and Experimental Nuclear Physics, Moscow, Russia

Forschungszentrum Karlsruhe
Institut für Materialforschung
Abteilung für Metallische Werkstoffe

1. Measurement of Average Recoil Ranges for Residual Nuclei from Alpha-Particle Induced Nuclear Reactions in Fe

E. Daum

At the Isochronous Cyclotron of the Forschungszentrum Karlsruhe alpha-particle induced nuclear reactions in a pure Fe target were investigated in the energy domain up to 104 MeV. The pre-compound and compound nuclear models describe the reaction mechanism in this energy region. After absorption of the projectile and emission of single nucleons or reaction fragments, a residual nucleus is left over which can have several MeV of kinetic energy. Thus the residual nucleus can move from its lattice site and travel a certain range. Due to the kinetics of the process the recoil momentum vector in the laboratory system is preferably directed downstream. In order to measure the average recoil ranges a special technique was applied [1]. Behind the high purity iron foil (≈ 16 µm) an aluminum foil was placed to catch the residual nuclei escaping from the iron foil. The average range can be calculated by the equation

$$R^{Nuc} = D\frac{A_C^{Nuc}}{A_C^{Nuc} + A_T^{Nuc}}$$

where R [µm] is the average range, D [µm] is the thickness of the target foil, A_T [Bq] is the specific activity of the nuclide *Nuc* in the target foil and A_C [Bq] is the specific activity in the catcher foil. The results are given in the table in [µm]. The uncertainty of the energy is due to the intrinsic uncertainty of the cyclotron and the uncertainty of the average range considering the thickness of the target foil and the statistical error of the gamma spectroscopic measurements.

E_α [MeV]	^{57}Ni	^{56}Ni	^{58}Co	^{57}Co	^{56}Co	^{55}Co	^{54}Mn	^{52}Mn	^{51}Cr	^{48}V
103,6 ± 0,7	0,66 ± 0,06	1,05 ± 0,47	0,59 ± 0,10	0,54 ± 0,05	0,77 ±0,05	0,91 ± 0,04	1,04 ± 0,10	1,07 ± 0,03	1,15 ± 0,06	1,17 ± 0,04
99,7 ± 1,0	0,74 ± 0,06	0,99 ± 0,30	0,60 ± 0,06	0,60 ± 0,03	0,75 ± 0,04	0,85 ± 0,05	0,93 ± 0,09	1,11 ± 0,04	1,12 ± 0,05	1,21 ± 0,04
95,4 ± 1,3	0,74 ± 0,04	0,93 ± 0,21	0,59 ± 0,04	0,61 ± 0,03	0,87 ± 0,04	0,80 ± 0,08	0,96 ±0,05	1,11 ± 0,04	1,10 ± 0,05	1,09 ± 0,04
91,0 ± 1,7	0,79 ± 0,06	1,04 ± 0,17	0,67 ± 0,03	0,68 ± 0,03	0,84 ± 0,03	1,03 ± 0,18	1,04 ± 0,05	1,15 ± 0,04	1,09 ± 0,05	1,10 ± 0,04
64,5 ± 0,7	0,62 ± 0,03	0,99 ± 0,39	0,70 ± 0,09	0,66 ± 0,04	1,14 ± 0,08	0,69 ± 0,04	0,74 ± 0,18	0,74 ± 0,03	1,34 ± 0,49	1,01 ± 0,48
54,4 ± 0,8	0,65 ± 0,03	0,52 ± 0,28	0,56 ± 0,08	0,56 ± 0,05	0,79 ± 0,06	0,62 ± 0,05	0,85 ± 0,13	0,77 ± 0,04	1,26 ± 0,42	
44,3 ± 0,9	0,54 ± 0,02	0,75 ± 0,37	0,74 ± 0,03	0,60 ± 0,02	0,49 ± 0,08	0,67 ± 0,03	0,70 ± 0,06	0,68 ± 0,03	0,86 ± 0,64	
34,2 ± 1,0	0,43 ± 0,02	0,88 ± 0,19	0,73 ± 0,02	0,35 ± 0,02	0,61 ± 0,05	0,46 ± 0,02	0,64 ± 0,02	0,29 ± 0,08		

References

[1] Alan Ewart, Constance Valentine and Marshall Blann, Nuclear Physics **69** (1965) 625-636
[2] E. Daum, FZKA-Bericht 5833, Forschungszentrum Karlsruhe (1996) 103-111

2. Calculation of Light Ion Induced Displacement Damage Cross Sections in Fe

E. Daum

In the framework of the characterization of displacement damage in iron under light ion irradiation, a comprehensive set of displacement damage cross section has been calculated in the energy domain up to 30 MeV for protons and up to 104 MeV for alpha-particles. This work concentrates on the non-elastic fraction of the displacement damage which is due to recoiling residual nuclei induced by nuclear reactions. For calculating the displacement damage cross sections, the primary knock-on spectra (PKA-spectra) and the secondary displacement function from the NRT-model the standard values for displacement energy in iron 40 eV and the displacement efficiency being 0.8 have been used. The displacement damage cross section is described by

$$\sigma_D(E) = \int \frac{d\sigma(E,T)}{dT} \nu(T) dT$$

where $d\sigma/dT\ (E,T)$ is the PKA-spectrum, $\nu(T)$ is the secondary displacement function and T is the PKA energy. The PKA-spectra were calculated with the nuclear model code ALICE [1]. A detailed description of the calculation procedure is given in [2, 3]. The displacement damage cross sections were calculated with protons for the nuclides ^{58}Co,^{57}Co,^{56}Co,^{55}Co, ^{53}Fe, ^{54}Mn, ^{52}Mn and with alpha-particles for the nuclides ^{57}Ni, ^{56}Ni, ^{58}Co,^{57}Co,^{56}Co,^{55}Co, ^{53}Fe, ^{52}Fe, ^{56}Mn, ^{54}Mn, ^{52}Mn, ^{51}Cr, ^{49}Cr, ^{48}V. The data can be found in [4]. Figure 1 shows as an example the non-elastic displacement damage cross section for the most important alpha-particle induced residual nuclei. In figure 2 the comparison between the elastic and the non-elastic displacement damage cross sections for high projectile energies shows that the non-elastic fraction is about 40% for alpha-particles and about 20% for protons.

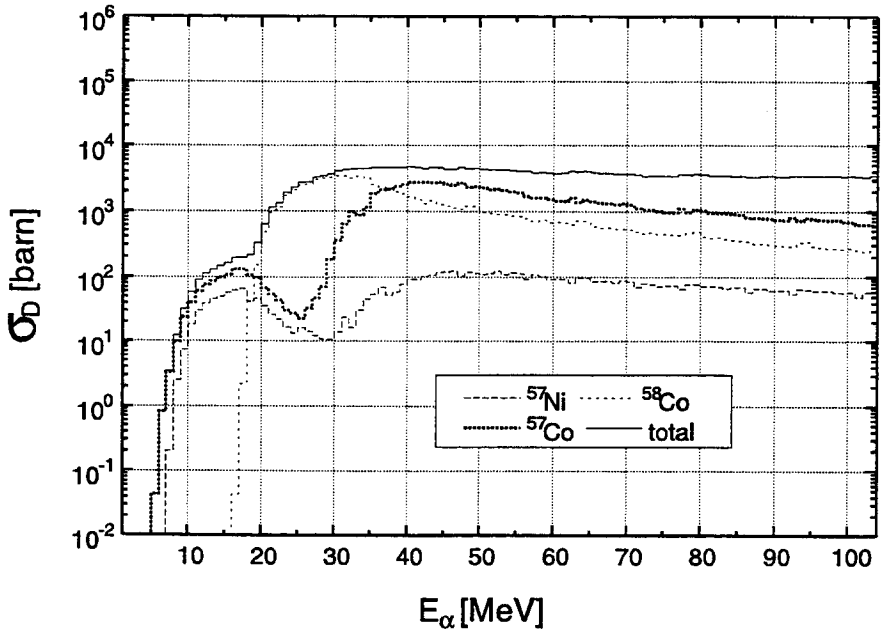

Figure 1 Alpha-particle induced non-elastic displacement damage cross sections in Fe.

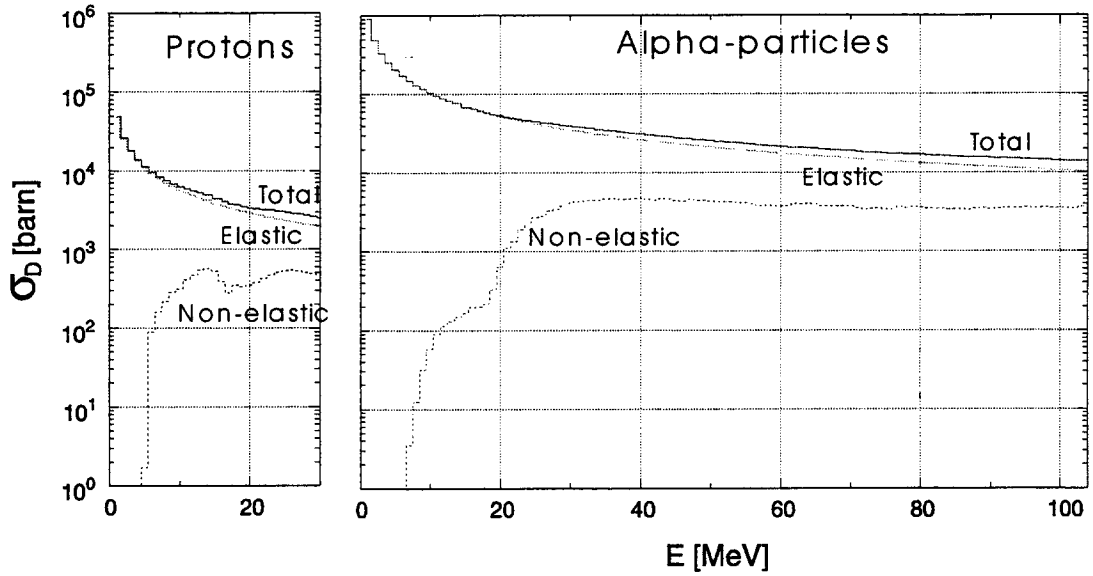

Figure 2 Comparison between the elastic and the non-elastic displacement damage cross sections for protons and alpha-particles in Fe.

References

[1] M. Blann, CODE ALICE/91, extended for recoil energies, private communication
[2] E. Daum, FZKA-Bericht 5833, Forschungszentrum Karlsruhe (1996)
[3] E. Daum, J. Bertsch, A. Möslang and K. Ehrlich, Journal of Nuclear Materials **233-237** (1996) 959-963
[4] E. Daum, FZKA-Bericht 5949, Forschungszentrum Karlsruhe (1997) 11-14

3. LINDA: A Computer Code for Calculation of Activation and Displacement Damage

E. Daum

In the framework of irradiation experiments at the Dual-Beam Facility of the Forschungszentrum Karlsruhe the question of the specimen activity and displacement damage in the specimen after a certain irradiation campaign appeared. Especially the fraction of the non-elastic displacement damage was of interest. The investigated targets were mainly iron based alloys. The Dual-Beam Facility can operate a H- and a He-beam at the same time. The energy domain is up to 30 MeV for protons and up to 104 MeV for alpha-particles. For a first step it was decided to concentrate only on the matrix element Fe. In order to gain predictions on the activation and non-elastic displacement damage for this setup the computer code LINDA (**L**ight **I**on induced **N**on-elastic **D**amage and **A**ctivation) and several databases as described above or in [1, 2, 3] were developed. LINDA is written in Fortran 77 and accesses an activation cross section database, a PKA-spectra database and a displacement damage cross section database. The activation cross section database consists of experimentally measured data and data calculated by the ALICE code [4]. The nuclear model data were fitted to the experimental data points throughout the whole energy domain of the Dual-Beam Facility. The PKA-spectra database was calculated as a function of the residual nuclei and the primary projectile energy with an extended ALICE version [5]. The displacement damage database was calculated from the PKA-spectra as described above. LINDA calculates using input parameters such as type of particle, primary energy, beam current, target thickness, irradiation time and decay time the number of produced nuclei, the activation, the surface gamma dose rate and the non-elastic displacements (DPA's) of a specimen as a function of the penetration depth. A special option is to calculate the parameters for the case of moderated primary energy from maximum energy down to 1 MeV. The output data are listed in tables. To make the use of LINDA computer platform independent, the Internet technology is used. A version of LINDA is implemented in conjunction with a WWW-Server. This LINDA version is accessible directly from the Internet and gives its results directly to the WWW-Browser from where it is started.

References

[1] E. Daum, FZKA-Bericht 5833, Forschungszentrum Karlsruhe (1996)
[2] S.M. Qaim (Ed.), NEA/NSC/DOC(97)13, INDC(Ger)-043, Jül-3410, Forschungszentrum Jülich, 1997
[3] E. Daum, FZKA-Bericht 5949, Forschungszentrum Karlsruhe (1997)
[4] M. Blann, CODE ALICE/85/300, UCID-20169, Lawrence Livermore National Lab., 1994
[5] M. Blann, CODE ALICE/91, extended for recoil energies, private communication

4. Measurement of the Impurity Concentration of Nb in the Japanese Steel F82H-mod by Activation Analysis

E. Daum , H.-D. Röhrig

Within the fusion technology program the development of low activation iron based alloys for structural components is a major activity. Activation calculations for candidate materials have shown that ^{93}Nb is a bad element regarding the long-term activation due to the long half-life of ^{94}Nb (20300 years) which is produced by neutron capture. This means that low activation steels only allow a very small residual concentration of ^{93}Nb. The Japanese reference alloy F82H-mod has been manufactured from pure ingot materials and has thus a very low niobium content of nominally 1 wt. ppm. In order to check this low niobium impurity concentration an activation experiment with 19.5 MeV alpha-particles on a 43 µm thin F82H-mod foil was carried out at the Isochronous Cyclotron of the Forschungszentrum Karlsruhe. The primary energy of 19.5 MeV was chosen because of a reasonable cross section prediction by the literature data. In order to get a good accuracy, reference measurements with high purity niobium and molybdenum foils were made at the same experimental setup. Molybdenum is located adjacent to niobium in the periodic table and causes in this experimental setup a major interference. The integral reference cross sections measured in the energy domain between 19.5 MeV and 14 MeV for Nb are σ(Nb $\rightarrow^{96}$Tc) = 46.4 mbarn (±8%) and in the energy domain between 19.5 MeV and 12 MeV for Mo are σ(Mo $\rightarrow^{96}$Tc) = 5.7 mbarn (±9%) and σ(Mo $\rightarrow^{97}$Ru) = 110.3 mbarn (±8%). The gamma spectroscopic analysis of F82H-mod yielded after correction for side reactions a niobium concentration of (2.5 ± 1.0) wt. ppm which is in good agreement with the manufacturer's data being 1 wt. ppm.

Reference

[1] E. Daum, H.-D. Röhrig, Journal of Nuclear Materials **250** (1997) 75-78

Forschungszentrum Karlsruhe
Institut für Neutronenphysik u. Reaktortechnik

Integral Data Tests, Sensitivity and Uncertainty Analyses for EFF Data Evaluations

U. Fischer, R. Perel [1], H. Tsige-Tamirat, E. Wiegner, Y. Wu [2]

In the framework of the European Fusion File (EFF) Project, a comprehensive programme of benchmark analyses has been conducted for the EFF data evaluations of Be, Si, Fe, Mo, Cr (EFF-2) and Al, Fe, and V (EFF-3). This included comparisons with corresponding nuclear cross-sections from the JENDL-FF (JAERI) and the FENDL-1 data files as well as data tests against integral experiments. Main results were presented in a contribution to the Int. Conf. On Nuclear Data for Science and Technology [1]. A comprehensive documentation with detailed results in numerical and graphical form is given Ref. 2.

Special attention was given to detailed analyses of the EFF-3 ^{56}Fe data. This evaluation shows advanced, unique features and was selected for that reason for FENDL-2. In particular, the EFF-3 ^{56}Fe evaluation includes a detailed and accurate description of the neutron total and inelastic cross-sections in the unresolved energy range above 0.85 MeV up to about 10 MeV based on ultra-high resolution cross section measurements performed at IRMM Geel [3]. The focus of the ^{56}Fe data test analyses was on the application of the data in MCNP based calculations for an iron slab experiment performed previously within the EFF-project at TU Dresden [4]. That experiment is typical for a fusion reactor shielding problem with pure iron and suitable for testing of iron cross section data. Measurements of neutron and photon spectra leaking from the 30 cm thick iron slab were provided in the experiment.

In the MCNP-calculations a full 3d-model, developed previously by TUD, of the experimental set-up was used including the neutron generator, collimator and the experimental hall. An anisotropic source distribution function was added to the model at FZK. In addition, two- and three-dimensional sensitivity and uncertainty calculations were performed to assess the uncertainties of the calculated neutron leakage flux spectra due to cross section uncertainties. The SUSD/TWODANT code package and covariance data processed from the EFF-2 and -3 data files was applied in the two-dimensional calculations [5]. A Monte-Carlo approach, developed recently at the University of Jerusalem [6], was used to conduct three-dimensional sensitivity and uncertainty calculations. This approach allows to obtain sensitivities and uncertainties for point detectors without restrictions in representing the geometry.

A comparison plot is shown in Fig. 1 for the neutron spectra, C/E (calculation over experiment) data are given for integrated neutron and photon fluxes in Fig. 2 and Table 1, respectively. It is concluded that there is generally good agreement with the measured neutron spectra within the experimental uncertainty for all of the state-of-the-art data files (EFF-2, -3, FENDL-1, JENDL-FF) and a clear improvement over obsolete data evaluations like EFF-1. The photon flux, however, in general is underestimated. With regard to EFF-3, there are two severe problems: one is the underestimation of the neutron spectrum in the energy range 5 - 10 MeV, the other one is the largely overestimated photon flux.

(1) *Permanent address: Racah Institute of Physics, Hebrew University of Jerusalem, 91904 Jerusalem, Israel*
(2) *Permanent address: Institute of Plasma Physics, Academia Sinica, P.O. Box 1126, Hefei, P.R. China*

Meanwhile both problems have been investigated in greater detail. It has been found that the first one isdue to an unsatisfactory evaluation of the secondary energy-angle distribution while the latter one was caused by an improper representation of the photon production data on the file with subsequent processing errors.

Table 1: C/E data for integrated photon flux spectra in the TUD iron slab experiment.

Energy range [MeV]	TUD experiment	C/E		
		EFF-3	EFF-2	FENDL-1
0.4 - 1.0	$(1.07 \pm 0.05)\cdot10^{-8}$	1.17	0.87	0.82
1.0 - 8.0	$(1.15 \pm 0.04)\cdot10^{-8}$	1.21	0.77	0.70
E > 0.4	$(2.22 \pm 0.10)\cdot10^{-8}$	1.19	0.81	0.76

With regard to the data uncertainties, the sensitivity and uncertainty calculations have shown a clear improvement of EFF-3 over the EFF-2 data. This is especially true for the uncertainties of the neutron fluxes in the different energy ranges (table 2). As for the uncertainties of the total neutron flux (E>0.1 MeV), there is involved a strong compensation of the uncertainties originating from elastic and inelastic neutron scattering. There remains an underestimation of the neutron flux above 5 MeV by about 10% which exceeds both the experimental and the calculated uncertainty. Note that the given calculated uncertainties are solely due to uncertainties in the excitation functions. Uncertainties coming from secondary energy and angle distributions are not yet included. When comparing the uncertainties calculated by the deterministic and the probabilistic approach, one can see that there is good agreement except for high energy (E> 10 MeV) component.

Table 2: Uncertainties [%] of calculated neutron fluxes in the TUD iron slab experiment due to cross section (excitation functions) uncertainties.

Energy range [MeV]	MC-calculation EFF-2.4	MC-calculation EFF-3.0	S_N-calculation EFF-3.0	Experimental uncertainty
<0,1	9	9	-	-
0.1-1	4	3	3	11
1 -5	20	1.6	2	2.2
5-10	27	8	10	2.9
>10	19	4	14	1.9
total	4	3	-	-

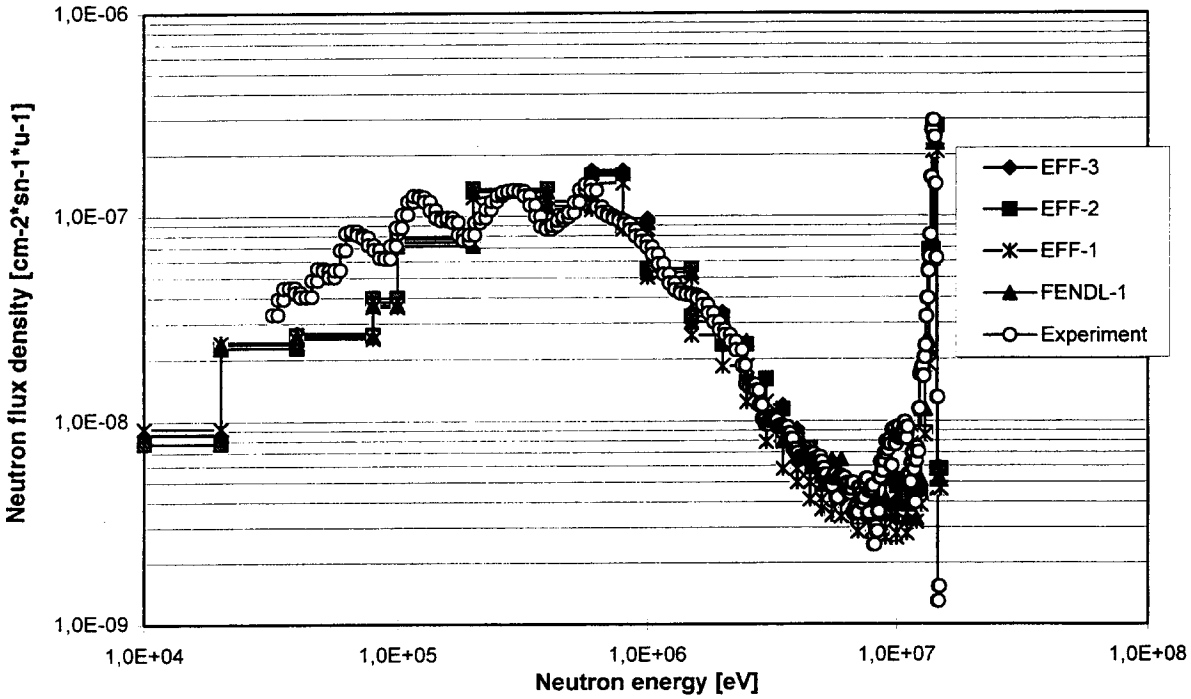

Fig. 1 Comparison of neutron flux spectra in TUD iron slab experiment

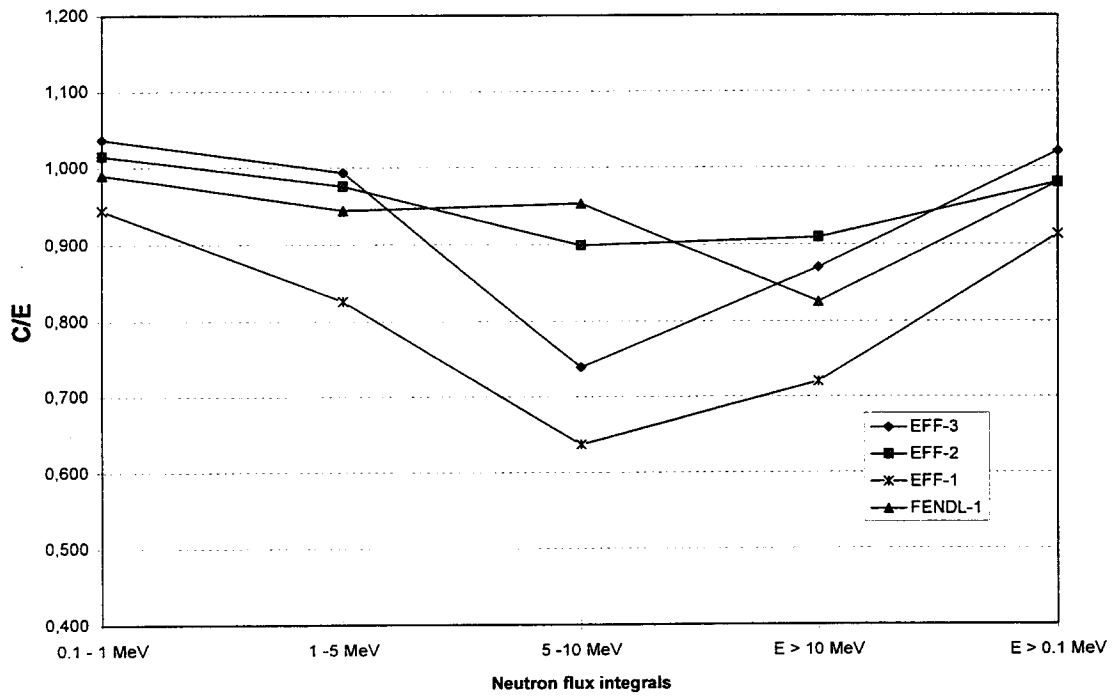

Fig. 2: C/E (Calculation/Experiment) - comparison for neutron flux integrals in the TUD iron slab experiment

References

[1] Y. Wu, U. Fischer, Integral Data Tests of the FENDL-1, EFF-2, EFF-3 and JENDL-FF Fusion Nuclear Data Libraries, in Proc. Nuclear Data for Science and Technology, edited by G. Reffo, A. Ventura and C. Grandi (Italian Physical Society, 1997), p. 1155

[2] Y. Wu, U. Fischer, Integral Data Tests of the FENDL-1, EFF-2, EFF-3 and JENDL-FF Fusion Nuclear Data Libraries Forschungszentrum Karlsruhe, Wissenschaftliche Berichte FZKA-5953, Februar 1998.

[3] K. Berthold, C. Nazareth, G. Rohr, H. Weigmann, Very high resolution measurements of the total cross section of natural iron, in Proc. Int. Conf. Nuclear Data for Science and Technology, edited by J. K. Dickens, American Nuclear Society, Inc. 1994, Volume 1, p. 218.

[4] H. Freiesleben et al., Experimental Results of an Iron Slab Benchmark, Technische Universität Dresden, TUD-PHY-94/2, February 1995.

[5] U. Fischer, H. Freiesleben, H. Klein, W. Mannhart, D. Richter, D. Schmidt, K. Seidel, S. Tagesen, H. Tsige-Tamirat, S. Unholzer, H. Vonach, Y. Wu, Application of Improved Neutron Cross Section Data for Fe-56 To An Integral Fusion Neutronics Experiment, in Proc. Nuclear Data for Science and Technology, edited by G. Reffo, A. Ventura and C. Grandi (Italian Physical Society, 1997), p. 1137

[6] R.L. Perel, J.J. Wagschal, and Y. Yeivin, "Monte Carlo Calculation of Point-Detector Sensitivities to Material Parameters", Nucl. Sci. Eng., **124** (1996), 197-209.

INSTITUT FÜR NUKLEARCHEMIE
FORSCHUNGSZENTRUM JÜLICH

1. Complex Particle Emission Reactions

M. Faßbender, B. Scholten, S.M. Qaim

In continuation of our fundamental studies on complex particle emission reactions [cf. 1] we extended the investigations on the (p,^{7}Be) process to proton energies up to 350 MeV, using the irradiation facilities at the THE SVEDBERG LABORATORY in Uppsala (Sweden) and the LABORATOIRE NATIONALE SATURNE, Saclay (France). Each irradiated foil was radiochemically processed and the weak ^{7}Be activity determined using a low-background HPGe detector. For most of the target nuclei the (p,^{7}Be) cross section over the energy range of 100 to 200 MeV was measured for the first time. At proton energies above 150 MeV, the excitation functions are practically constant. For an incident energy of 180 MeV, the reaction cross section was plotted as a function of mean mass number (A) of the target element. The results are depicted in Fig. 1. Evidently, the (p,^{7}Be) cross section decreases rapidly with the increasing mass number of the element [cf. 2].

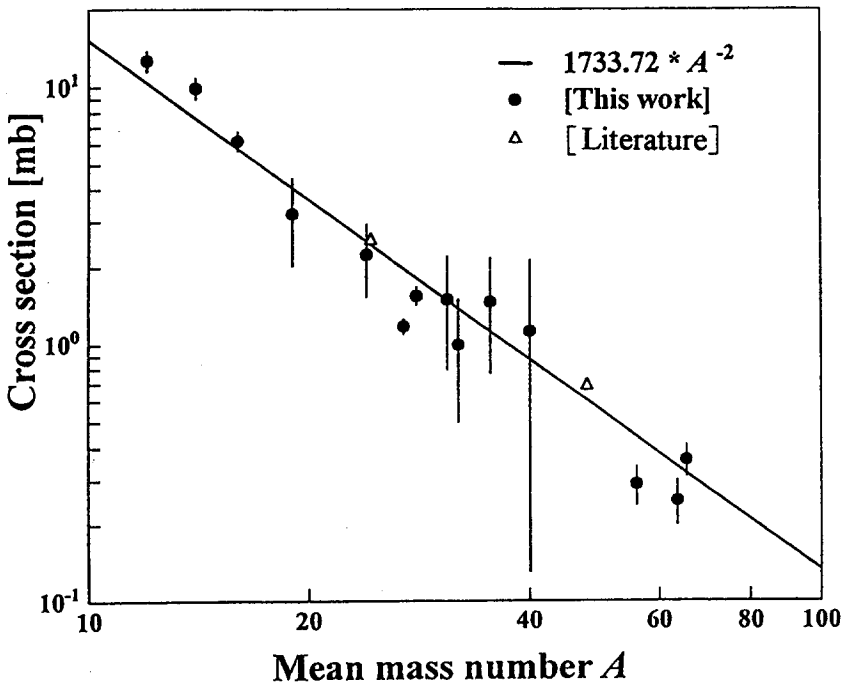

Fig. 1 (p,^{7}Be) cross section at E_p = 180 MeV as a function of mean mass number (A) of the target element (for details cf. [2]).

2. Isomeric Cross Sections

C. Nesaraja, R. Dóczi*, F. Cserpák*, S. Sudar*, J. Csikai*, A. Fessler†, B. Strohmaier††, S.M. Qaim

Some of the on-going experimental and theoretical studies on this topic were completed [cf. 3 - 6]. Of special interest are the results on ^{69m,g}Zn, ^{94m,g}Tc and ^{89m}Y. The formation of the isomeric pair ^{69m,g}Zn was investigated in ^{70}Zn(n,2n)-, ^{69}Ga(n,p)- and ^{72}Ge(n,α)-processes over the energy range of 5 to 15 MeV. The particle emitted in the exit channel did not show any significant effect on the isomer ratio. The isomeric pair ^{94m,g}Tc, on the other hand, was studied in ^{94}Mo(p,n)-, ^{93}Nb(^{3}He,2n)- and ^{92}Mo(α,pn)-reactions, and the isomer ratio was found to be strongly dependent on the type of projectile used. In both the cases, nuclear model calculations based on the code STAPRE reproduced the experimental data well. The third case, i.e. the formation of ^{89m}Y, involved measurements and calculations on the ^{89}Y(n,n'γ)-process.

Over the neutron energy range of 5 to 12 MeV, very few isomeric states populated in the (n,n'γ) process have been investigated, mainly due to the problem of high neutron background. Using an improved D-D neutron source and a method for background correction we obtained the data given in Fig. 2. The good agreement between experiment and theory over the whole investigated energy range suggests that the activation technique can be applied also to the study of a low threshold reaction, provided the contributions of various neutron components in the quasi-monoenergetic neutrons are carefully treated [cf. 6].

Other investigations on the isomeric cross sections were related to the formation of high spin states ^{53m}Fe ($I = 19/2^-$), ^{195m}Hg ($I = 13/2^+$) and ^{197m}Hg ($I = 13/2^+$) in (n,2n), (^{3}He,2n) and (α,2n) processes. Data analysis and nuclear model calculations are in progress.

---

* Institute of Experimental Physics, Kossuth University, Debrecen, Hungary
† Mainly at IRMM, Geel, Belgium
†† Institut für Radiumforschung und Kernphysik, Universität Wien

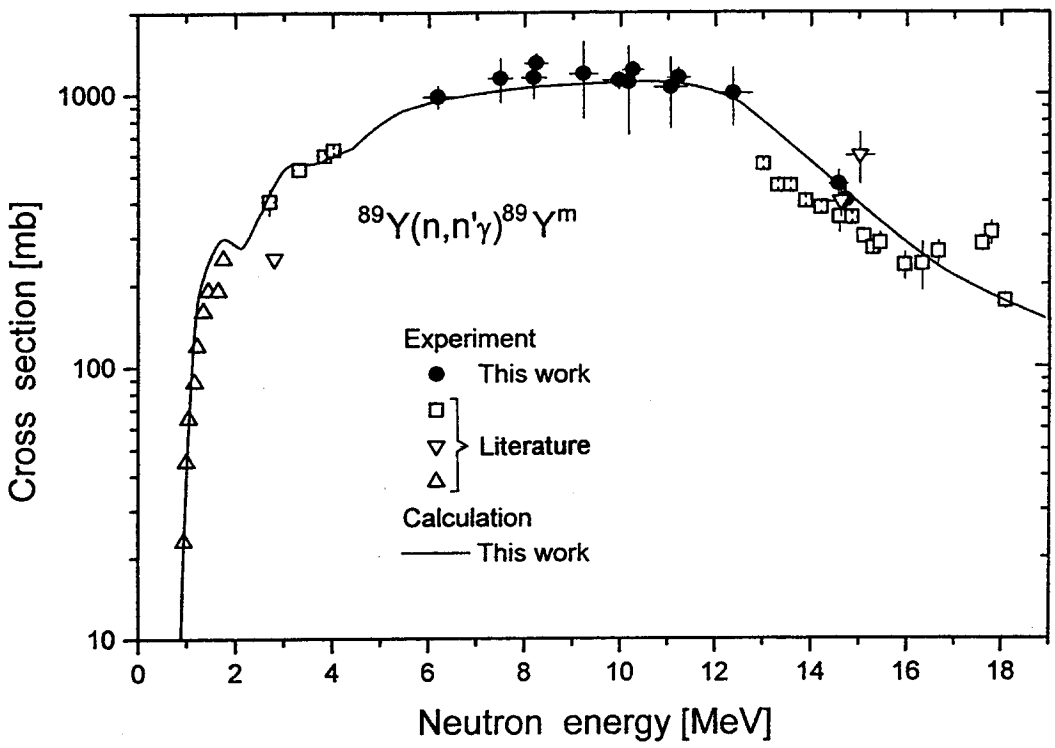

Fig. 2 Measured and calculated excitation function of the $^{89}Y(n,n'\gamma)^{89m}Y$ reaction (for details cf. [6]).

3. Neutron Activation Cross Sections

C. Nesaraja, S. Spellerberg, F. Cserpák*, S. Sudár*, J. Csikai*, A. Fessler†, S.M. Qaim

(Relevant to request identification numbers: 92 10 04 F, 92 10 09 M, 92 10 56 R, 92 10 68 R, 92 10 69 R, 92 30 77 F)

Cross sections were measured for the $^{52}Cr(n,p)^{52}V$, $^{53}Cr(n,p)^{53}V$ and $^{54}Cr(n,p)^{54}V$ reactions in the energy range of 9 to 12 MeV at Jülich and 15 to 21 MeV at IRMM Geel, Belgium, in collaboration with E. Wattecamps and D.L. Smith. The data were compared with the results of nuclear model calculations based on the code STAPRE-H and the agreement was found to be good. Using the present and literature data, some systematic trends in the excitation functions of (n,p) reactions were analysed (for more details cf. Ref. [7]).

---

* Institute of Experimental Physics, Kossuth University, Debrecen, Hungary
† Mainly at IRMM, Geel, Belgium

Excitation functions of the following reactions were measured in the neutron energy range of 6 to 12 MeV: $^{67}Zn(n,p)^{67}Cu$, $^{68}Zn(n,\alpha)^{65}Ni$, $^{70}Ge(n,p)^{70}Ga$, $^{109}Ag(n,p)^{109m+g}Pd$. Some of the results have already been described [cf. 4] and a more detailed report is in preparation. Most of the data have been determined for the first time. Nuclear model calculations were done using the code STAPRE. The results were found to be strongly dependent on the input parameters: *a priori* calculations seldom reproduce the experimental data quantitatively.

Special attention was paid to the investigation of the $^{58}Ni(n,\alpha)^{55}Fe$ and $^{50}Cr(n,n'p)^{49}V$ processes. In the former case a discrepancy exists between an earlier activation measurement done at Jülich and the emitted α-particle detection carried out elsewhere (cf. E. Wattecamps, Nucl. Data for Science and Technology, edited by S.M. Qaim, Springer Verlag, Berlin, 1992, p. 310). The latter reaction has hitherto not been investigated. Both the reactions have a common feature: the products decay by EC and emit soft x-rays which are difficult to characterize. For the present measurements, irradiations were done at Jülich and Geel, the radioactive products were isolated by elaborate radiochemical separations, and thin sources were prepared. The radioactivity was then determined by soft x-ray spectrometry. The data analysis is in progress.

4. Excitation Functions Relevant to Radioisotope Production

A. Hohn, P. Reimer, A. Klein, S. Kastleiner, E. Heß, F. Tárkányi*, S.Takács*, Z. Szücs*, B. Scholten, H.H. Coenen, S.M. Qaim

In continuation of our systematic studies on data for medical applications [cf. 8 - 11], during the period of the present report measurements were carried out in connection with the following types of radioisotopes:

a) *Short-lived positron emitters*. The data for the production of the four major β^+ emitters (^{11}C, ^{13}N, ^{15}O, ^{18}F) are fairly well known; only in a few cases some

---

* Institute of Nuclear Research of the Hungarian Academy of Sciences (ATOMKI), Debrecen, Hungary

additional information is desired. During the production of ^{15}O via the $^{14}N(d,n)$-process, for example, small amounts of ^{13}N and ^{11}C are also formed, but the cross sections of the contributing processes were not known with high accuracy. We measured the excitation functions of the $^{14}N(d,t)^{13}N$ and $^{14}N(d,\alpha n)^{11}C$ reactions from their respective thresholds up to 12.3 MeV. Using the experimental data the yields of the two products were calculated and then the ratio of the impurity (^{13}N or ^{11}C) to ^{15}O was determined. The results are shown in Fig. 3. Evidently, at deuteron energies above 10 MeV the amounts of the impurities increase rapidly [12]. This information is essential with regard to the disposal of waste gases.

A second example is the $^{18}O(p,n)^{18}F$ reaction which is the most commonly used process for the production of ^{18}F (as fluoride). There are some discrepancies in the data measured by the activation and neutron detection techniques. We performed some measurements over the energy range of 10 to 20 MeV. Further measurements near the threshold of the reaction and data analysis are in progress.

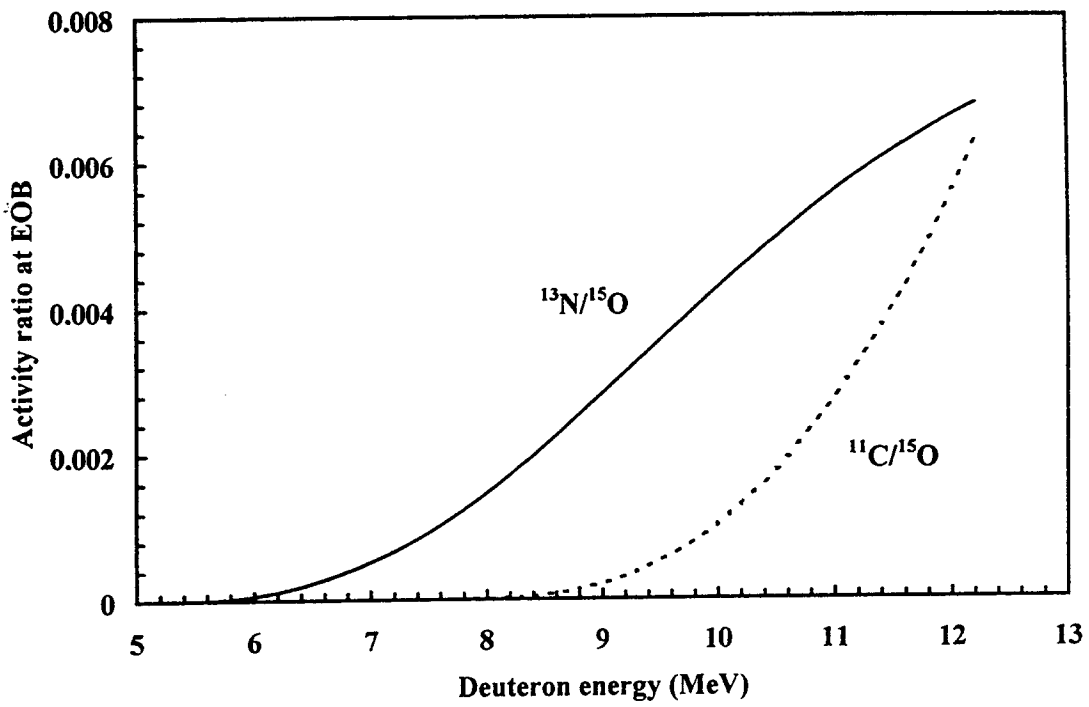

Fig. 3 Activity ratio of ^{13}N and ^{11}C to ^{15}O (at EOB) as a function of deuteron energy on the N_2 gas target. The values were calculated from the cross section data measured in this work (for details cf. [12]).

b) *Positron emitting radioisotopes of iodine.* For quantitative evaluation of radio-iodopharmaceuticals via Positron Emission Tomography (PET), some suitable β^+ emitting radioisotope of iodine is needed. The radioisotope ^{124}I ($T_{½}$ = 4.15 d; $E_{\beta+}$ = 1.8 MeV; $I_{\beta+}$ = 25 %) has found some application. It is generally produced via $^{124}Te(p,n)$- and $^{124}Te(d,2n)$- processes; the yields in both cases, however, are rather low. Since the $^{125}Te(p,2n)^{124}I$ and $^{126}Te(p,3n)^{124}I$ reactions using medium energy protons appear to be promising, we started a study of those processes. More interesting, however, is the radioisotope ^{120g}I ($T_{½}$ = 1.35 h; $E_{\beta+}$ = 4.0 MeV; $I_{\beta+}$ = 46 %). In the last Progress Report we described cross section measurements on the $^{122}Te(p,3n)^{120m,g}I$ processes. It was found that the energy range $E_p = 37 \rightarrow 32$ MeV is very suitable for production purposes [13]. The major drawback of the method is the rather high-level of the isomeric impurity ^{120m}I (~ 25 %). Now we investigated the $^{120}Te(p,n)^{120m,g}I$ processes using highly enriched ^{120}Te as the target material [14]. The results are reproduced in Fig. 4. Whereas the cross section of the

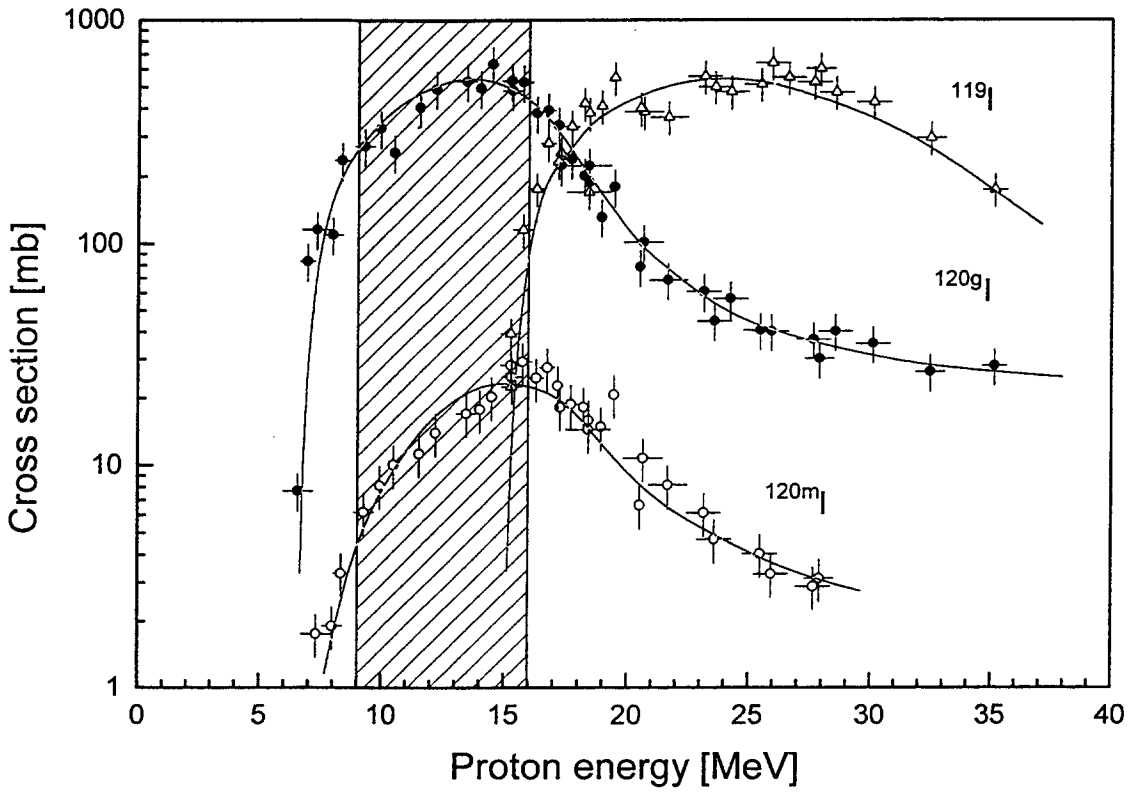

Fig. 4 Excitation functions of $^{120}Te(p,xn)$-reactions leading to the formation of ^{120m}I, ^{120g}I and ^{119}I. The solid lines are eye-guides. The shaded area gives the optimum energy range for the production of ^{120g}I (for details cf. [14]).

$^{120}Te(p,n)^{120g}I$ reaction is fairly high, that of the $^{120}Te(p,n)^{120m}I$ process is rather low. Thus, over the optimum energy range E_p =16 → 9 MeV the thick target yield of ^{120g}I amounts to 2.3 GBq (62 mCi/μAh) and the ^{120m}I impurity level to 4.8 %. The method is thus very suitable for the production of ^{120g}I. An added advantage is that a small-sized cyclotron is adequate for production purposes. The major disadvantage, on the other hand, is the high cost of the target material.

c) *Other radioisotopes*. Measurements on the $^{100}Mo(p,2n)^{99m}Tc$, $^{100}Mo(p,pn)^{99}Mo$ and $^{98}Mo(p,\gamma)^{99m}Tc$ processes, initiated last year under a technical contract with the IAEA and in collaboration with R.M. Lambrecht (Tübingen) and M. Cogneau (Louvain-la-Neuve, Belgium), were completed [15]. The results show that the $^{100}Mo(p,2n)^{99m}Tc$ reaction can be used for regional production of ^{99m}Tc ($T_{½}$ = 6.0 h) at a cyclotron with E_p > 17 MeV. For ^{99}Mo-^{99m}Tc generator production the $^{100}Mo(p,pn)^{99}Mo$ process is not viable due to low yields. The reactor production of ^{99}Mo thus remains the method of choice.

The therapy related radioisotope ^{67}Cu ($T_{½}$ = 61.9 h; E_{β^-} = 0.58 MeV; I_{β^-} = 100%) is either produced via the $^{68}Zn(p,2p)^{67}Cu$ process at $E_p \geq 100$ MeV or via the $^{67}Zn(n,p)^{67}Cu$ reaction using reactor neutrons. We investigated the $^{70}Zn(p,\alpha)^{67}Cu$ reaction from its threshold up to 35 MeV, using 85% enriched ^{70}Zn. Although the cross section is not very high, ^{67}Cu yields of about 3 MBq (80 μCi/μAh) could be obtained over E_p = 20 → 7 MeV. The method could serve as an alternative route for production of small amounts of ^{67}Cu. Although the target material ^{70}Zn is rather expensive, the advantage of the method is that a small-sized cyclotron would be adequate for production purposes.

References (Publications from Jülich during the Period of the Progress Report)

[1] S. Merchel, S.M. Qaim: Excitation functions of (^3He,^7Be)-reactions on light mass target elements, Radiochimica Acta 77 (1997) 137

[2] M. Faßbender, B. Scholten, S.M. Qaim: Radiochemical studies of (p,^7Be) reactions on biologically relevant elements in the proton energy range of 50 to 350 MeV, Radiochimica Acta, in press

[3] B. Strohmaier, M. Faßbender, F.-O. Denzler, F. Rösch, S.M. Qaim: Isomeric cross section ratio for the formation of ^{94m,g}Tc in various charged-particle induced reactions, in Nuclear Data for Science and Technology (G. Reffo, A. Ventura, C. Grandi, editors), Italian Physical Society, Vol. 59 (1997) p. 287

[4] C. Nesaraja, F. Cserpák, S. Sudár, R. Dóczi, S.M. Qaim: Excitation functions of (n,p) and (n,α) reactions on some isotopes of Zn, Ge, Y and Ag, *ibid*, p. 583

[5] B. Strohmaier, M. Faßbender, S.M. Qaim: Production cross sections of ground and isomeric states in the reaction systems ^{93}Nb + ^{3}He, ^{92}Mo + α and ^{94,95}Mo + p, Phys. Rev. C56 (1997) 2654

[6] R. Dóczi, S. Sudár, J. Csikai, S.M. Qaim: Excitation functions of the ^{89}Y(n,n'γ)^{89m}Y and ^{89}Y(n,α)^{86m}Rb processes, Phys. Rev. C, submitted

[7] A. Fessler, E. Wattecamps, D.L. Smith, S.M. Qaim: Excitation functions of (n,2n), (n,p), (n,np + pn + d) and (n,α) reactions on isotopes of chromium, Phys. Rev. C, in press

[8] M. Faßbender, B. Scholten, Yu. N. Shubin, S.M. Qaim: Activation cross section data for (p,x) processes of therapeutic relevance, in Nuclear Data for Science and Technology, as in Ref. [3], p. 1646

[9] M. Faßbender, Yu. N. Shubin, V.P. Lunev, S.M. Qaim: Experimental studies and nuclear model calculations on the formation of radioactive products in interactions of medium energy protons with copper, zinc and brass: Estimation of collimator activation in proton therapy facilities, Appl. Radiat. Isotopes 48 (1997) 1221

[10] A. Fenyvesi, S. Merchel, S. Takács, F. Szelecsényi, F. Tárkányi, S.M. Qaim: Excitation functions of ^{nat}Ne(^{3}He,x)^{22,24}Na and ^{nat}Ne(α,x)^{22,24}Na processes: Investigation of production of ^{22}Na and ^{24}Na at a medium-sized cyclotron, Radiochimica Acta 79 (1997) 207

[11] P. Reimer, S.M. Qaim: Excitation functions of proton induced reactions on highly enriched ^{58}Ni with special relevance to the production of ^{55}Co and ^{57}Co, Radiochimica Acta 80 (1998) 113

[12] Z. Szücs, W. Hamkens, S. Takács, F. Tárkányi, H.H. Coenen, S.M. Qaim: Excitation functions of ^{14}N(d,t)^{13}N and ^{14}N(d,αn)^{11}C reactions from threshold to 12.3 MeV: Radionuclidic purity of ^{15}O produced via the ^{14}N(d,n)^{15}O reaction, Radiochimica Acta 80 (1998) 59

[13] A. Hohn, B. Scholten, H.H. Coenen, S.M. Qaim: Excitation functions of (p,xn)-reactions on highly enriched ^{122}Te: Relevance to the production of ^{120g}I, Appl. Radiat. Isotopes 49 (1998) 93

[14] A. Hohn, H.H. Coenen, S.M. Qaim: Nuclear data relevant to the production of ^{120g}I via the ^{120}Te(p,n)-process at a small-sized cyclotron, Appl. Radiat. Isotopes, in press

[15] B. Scholten, R.M. Lambrecht, M. Cogneau, H. Vera Ruiz, S.M. Qaim: Excitation functions for the cyclotron production of ^{99m}Tc and ^{99}Mo, Appl. Radiat. Isotopes, submitted

INSTITUT FÜR KERN- UND TEILCHENPHYSIK TECHNISCHE UNIVERSITÄT DRESDEN

1. Integral Activation Experiment with 14 MeV Neutrons on Vanadium Alloys*

K. Seidel, R. A. Forrest[a], H. Freiesleben, V. D. Kovalchuk[b], D. V. Markovskij[c], D. Richter, V. I. Tereshkin[b], S. Unholzer

Vanadium alloys are potential structural materials for fusion reactors, especially because of their low-activation behaviour. In the present work the radioactivities induced by 14-MeV neutrons in V3Ti1Si, V4Ti4Cr and V5Ti2Cr are experimentally investigated. In addition to producing data on the specific alloys, the aim of detailed analyses of the activities measured is the validation of the calculational tools - the European Activation System (EASY) [1] - for this class of materials.

Small samples (area of about 10 x 10 mm and mass of 0.3 ... 0.6 g) of the alloys were irradiated at the high-intensity neutron generator SNEG-13 at Sergiev Posad [2]. The expected activation profile suggested to make two separate irradiations, a short one (30 min) with fluence of about 6 x 10^{11} neutrons cm^{-2} and a longer one (45.6 h) with fluence of about 2 x 10^{14} neutrons cm^{-2}. In this way, radioactivities with half-life between 2 min and more than 300 d could be investigated.
Gamma spectra were taken from the irradiated samples with a Ge(Li)-spectrometer several times during cooling from 3 min up to about 100 d. The activities of the following nuclides were identified by gamma energies and half-life: ^{24}Na, ^{27}Mg, ^{28}Al, ^{29}Al, ^{46}Sc, ^{47}Sc, ^{48}Sc, ^{45}Ti, ^{51}Ti, ^{52}V, ^{51}Cr, ^{54}Mn, ^{57}Co, ^{58}Co, ^{95}Zr, ^{92m}Nb and ^{99}Mo. These nuclides produce after 3 min of cooling more than 99% of the total heat and of the gamma dose rate, and after 1 year of cooling, when the activity of the sample is further decreased by almost 6 orders of magnitude, they are the origin of about 92% of the heat and of more than 99% of the gamma dose rate. For each of the activities measured, calculations with EASY-97 (inventory code FISPACT and European Activation File as data base, version 1997) were carried out, and ratios of calculated-to-experimental values (C/E) were derived.

The values obtained for the activities with short half-life are shown in Table 1. Validation of EASY-97 was found for most of the activities (marked by *) if the total uncertainties of the C/E, including besides the experimental uncertainties also the calculational one (cross-section and half-life uncertainties), are used with one standard deviation as a measure. The C/E data in the third column are the averages obtained for the activity from the independently investigated alloys using the bold numbers. The range of these extracted results includes the experimental uncertainty only. The reactions contributing to the activities are presented in Table 2 for further analysis, especially those with larger deviations from unity.

References

[1] R.A. Forrest, J-Ch. Sublet, J. Kopecky, The European Activation System (EASY), Int. Conf. On Nuclear Data for Science and Technology, Trieste, 19-24 May 1997, Proc. P. 1140.
[2] V.D. Kovalchuk et al., Neutron generator SNEG-13, Report IAE-5589/8, RCC Kurchatov Institute, Moscow, 1992.

* Work supported by the European Fusion Technology Programme

[a] UKAEA Fusion, Culham, Abingdon OX143DB, United Kingdom
[b] Coordination Centre „Atomsafety" Sergiev Posad, 141300 Moscow Reg., Russia
[c] Russian Research Centre „Kurchatov Institute", 123182 Moscow, Russia

Table 1: Calculated-to-experimental activities

Nuclide	Half-life	*Gamma lines / keV*	C/E - values C/E - uncertainties (exp., calc., total) in %			**C/E extracted** exp. unc. range
			V4Cr4Ti	**V5Ti2Cr**	**V3Ti1Si**	
^{27}Mg	9.46min	*844*	0.65* (51., , >51.)			
^{28}Al	2.25min	*1779*	0.92* (43.,23.,49.)	**0.75*** (**18.**,24.,30.)	**0.80*** (**18.**,24.,30.)	**0.78** **(0.65...0.90)**
^{29}Al	6.6min	*1273*			1.29* (49., ,>49)	
^{47}Sc	3.35d	*159*	**1.65*** (**14.**,35.,37.)	2.04* (36.,35.,51.)	2.69 (39.,33.,51.)	**1.65** **(1.42...1.88)**
^{48}Sc	43.67h	*175, 984, 1038, 1312*	**1.14*** (**8.8**,27.,28.)	**0.95*** (**15.**,26.,30.)	**1.04*** (**12.**,28.,30.)	**1.04** **(0.95...1.13)**
^{45}Ti	3.08h	*511*	**1.25*** (**18.**,39.,43.)	**0.95*** (**21.**,40.,45.)	**1.32*** (**23.**,40.,46.)	**1.17** **(1.00...1.34)**
^{51}Ti	5.8min	*320, 609, 928*	**1.20*** (**8.6**,30.,31.)	**0.97*** (**11.**,30.,32.)	**1.06*** (**10.**,30.,32.)	**1.08** **(1.01...1.15)**
^{52}V	3.75min	*1443*	**0.91*** (**8.9**,21.,23.)	0.60 (12.,22.,26.)		**0.91** **(0.83...0.99)**

Table 2: Reactions contributing to the production of the activities

Nuclide	Half-life	C/E extracted	Reactions contributing (V4Ti4Cr)	
^{28}Al	2.25min	0.65.....0.90	^{28}Si(n,p) ^{31}P(n,a)	97.70% 1.75%
^{47}Sc	3.35d	1.42.....1.88	^{47}Ti(n,p) ^{48}Ti(n,d) ^{50}V(n,a) ^{51}V(n,na)	24.13% 43.25% 5.60% 26.81%
^{48}Sc	43.67h	0.95.....1.13	^{48}Ti(n,p) ^{51}V(n,a)	10.57% 89.26%
^{45}Ti	3.08h	1.00.....1.34	^{46}Ti(n,2n)	100%
^{51}Ti	5.8min	1.01.....1.15	^{51}V(n,p)	99.95%
^{52}V	3.75min	0.83.....0.99	^{51}V(n,g) ^{52}Cr(n,p) ^{53}Cr(n,d)	18.93% 78.20% 2.58%

2. Measurement of Nuclear Heating in a Fusion Reactor Blanket Mock-up by a Silicon Micro-sensor*

H. Freiesleben, D. Richter, K. Seidel, S. Unholzer

The useful energy produced by a fusion reactor is mainly kinetic energy of neutrons that is converted in the blanket system into heat. To a great extend this energy deposition is effected by atomic collisions of the gamma-rays produced by nuclear interactions of the neutrons. Amount and distribution of heat in the blanket components belong to the central parameters of the reactor layout. For the design of the International Thermonuclear Experimental Reactor (ITER) the heating performance was experimentally investigated. A neutronic mock-up at the Frascati neutron generator simulates the ITER inboard shield including first wall, shielding blanket, vacuum vessel and toroidal field coils [1]. Irradiated with 14 MeV neutrons, the total neutron flux is attenuated in this bulk assembly (thickness: about 100 cm) by more than five orders of magnitude. Heating measurements had to be performed along a central axis of the mock-up.

Complementary to heating measurements with thermoluminescent dosimeters (TLD) [2], a silicon sensor was used at two positions, A and B, for which the neutron and gamma flux spectra had already been measured [3]. Position A was located at about half of the assembly thickness, and position B at the rear part where the neutron and gamma fluxes have the lowest values. The sensor (from VACUTEC Messtechnik GmbH, Dresden) has a very compact layout needed for in-core measurements. A hybrid circuit includes Si-pin-diode, charge-sensitive preamplifier and discriminator. For additional enhancing the sensitivity the detector was not operated as current chamber but pulses were acquired [4]. The pulse-height spectra measured were experimentally corrected for events induced by neutron interactions in the detector.

The gamma-heating values obtained by the Si-sensor are compared in Table 1 with both, experimental TLD results and data from the measured gamma flux spectra multiplied by KERMA factors derived from the FENDL-1 transport library [5]. Taking into account that the flux spectra were determined for a spherical volume with radius of 2.0 cm, whereas the TLD and the Si detector had very much smaller volumes, which results in slightly reduced values in the case of flux measurements because of averaging over the detector volume, and taking into account the slightly different positions of the TLD measurements, consistency can be stated.

Table 1: Comparison of the measured gamma heating with other experimental and with calculated results

	Gamma dose / (10^{-17} Gy / source neutron) at Position A		Gamma dose / (10^{-19} Gy / source neutron) at Position B	
This work	8.58±0.86	(z = 41.5cm)	1.45±0.19	(z = 87.6cm)
TLD measurement by ENEA [2]	7.04±0.61	(z = 41.9cm)	1.15±0.15	(z = 88.0cm)
Spectral gamma flux measurement by TUD [4] plus KERMA data of FENDL-1	7.39±0.33	(z = 41.5cm)	1.06±0.06	(z = 87.6cm)
Calculation ENEA [2] (FENDL-1 data) extrapolated to the Si-Sensor position	7.15 7.55	(z = 41.9cm) (z = 41.5cm)	0.893 0.933	(z = 88.0cm) (z = 87.6cm)

The heating values calculated with ITER design tools, the three-dimensional Monte Carlo code MCNP-

* Work supported by the European Fusion Technology Programme

4A [6] and the FENDL-1 data library, are included in Table 1, too. Whereas for position A the underestimation is only marginal, it is significant for position B, where the ratio of calculated-to-experimental value amounts to 0.64 (±13% experimental uncertainty). This underestimation is mainly caused by the calculated gamma flux, but not by the KERMA data. The reason for the underestimated gamma flux again, has been found to be attributed to the neutron flux at deep penetrations [3].

References

[1] P. Batistoni et al., Neutronics shield experiment for ITER at the Frascati neutron generator, Proceedings of the 19th Symposium on Fusion Technology, Lisbon, Portugal, 16-20 September 1996, Fusion Technology 1996, C. Varandas and F. Serra (editors), 1997 Elsevier Science B. V., p. 233.
[2] P. Batistoni, M. Angelone, L. Petrizzi, M. Pillon, M. Gallina, Nuclear heating measurements and analysis in the bulk shield experiment, ITER Task T218/ ENEA, Report, ENEA Frascati, June 1996.
[3] U. Fischer et al., Investigation of spectral neutron and gamma fluxes in a fusion reactor blanket mock-up, Progress Report on Nuclear Data Research in the Federal Republic of Germany, ed. by S. M. Qaim, NEA/NSC/DOC(97)13, INDC(GER)-043, p. 26, Jülich 1997.
[4] H. Freiesleben et al., Measurement of nuclear heating by a silicon micro-sensor in the ITER bulk shield experiment, Report TU Dresden, Institut für Kern- und Teilchenphysik, TUD-IKTP-97/4, Nov. 1997.
[5] S. Ganesan, P. K. Mc Laughlin, FENDL/E - Evaluated nuclear data library of neutron interaction cross sections, photon production cross sections and photon-atom interaction cross sections for fusion applications, Version 1.0, Report IAEA-NDS-128, Vienna, 1994.
[6] J. F. Briesmeister (ed.), MCNP- A general Monte Carlo n-particle transport code, Version 4A, Report LA-12625-M, Los Alamos, 1993.

3. Approximation Formula for K Series X-Ray Energies

G.Beulich, G.Zschornack

For quantitative x-ray analysis with modern wavelength or energy dispersive spectrometers, precise x-ray data such as line energies (wavelengths) and intensity ratios for relevant transitions are needed. Compilations of experimental and evaluated data [1-4] result in extensive files. However, empirical equations, which fit the numerous data with only a few parameters are useful for many applications. For the element identification, the x-ray energies are needed with a precision of the order of eV.
In the present work all important x-ray lines of the K series for atomic numbers Z ranging between 13 ≤ Z ≤ 92 were fitted by the least-squares method with the seven-parameter expression

$$E = \sum_{k=0}^{6} a_k Z^k \quad . \tag{1}$$

For improving the approximation separate fits for Z _ 50 and for Z _ 50 were carried out. The parameters obtained are presented in Table 1. The differences between experimental x-ray energies and the corresponding values calculated with Eq. (1) are shown in Fig. 1 for the $K_{\alpha 1}$ transitions and in Fig. 2 for the $K_{\beta 1}$ transitions. They are of the order of eV for Z < 80, or within the error bars of the experimental data. The x-ray energies calculated with an approximation published by Norrish and Tao [5] are also included in the figures as difference to the present formula. Norrish and Tao extracted their parameters from fits to the experimental data for 11 ≤ Z ≤ 72 without splitting the fit range. The deviations are clearly larger.

Obviously, the aim of the present work, the description of the x-ray energies with a precision of the order of eV, was achieved by splitting the Z range.

Table 1: Coefficients for the numerical approximation of strong K series x-ray transition energies by Eq. (1).

line	$K_{\alpha 1}$	$K_{\alpha 1}$	$K_{\alpha 2}$	$K_{\alpha 2}$
transition	K-L_3	K-L_3	K-L_2	K-L_2
Z-region	13-51	52-92	13-51	52-92
a_0	-31.8	-10.6	-102.5	-6.0
a_1	4.245	-121.969	20.02	-69.168
a_2	7.17411	18.47846	5.79605	14.55659
a_3	0.1621729	-0.2697796	0.2228508	-0.1534255
a_4	$-4.44307\ 10^{-3}$	$4.42847\ 10^{-3}$	$-5.886018\ 10^{-3}$	$2.672466\ 10^{-3}$
a_5	$6.40876\ 10^{-5}$	$-3.36854\ 10^{-5}$	$8.06826\ 10^{-5}$	$-2.089145\ 10^{-5}$
a_6	$-3.43902\ 10^{-7}$	$1.12316\ 10^{-7}$	$-4.24058\ 10^{-7}$	$7.17875\ 10^{-8}$
line	$K_{\beta 1}$	$K_{\beta 1}$	$K_{\beta 3}$	$K_{\beta 3}$
transition	K-M_3	K-M_3	K-M_2	K-M_2
Z-region	15-51	52-92	29-59	60-92
a_0	368.2	260.0	-2.3	0
a_1	-112.231	31.057	-15.574	0.606
a_2	18.71065	8.49654	10.2575	9.01638
a_3	-0.3238662	0.0356847	0.03056	0.0638394
a_4	$7.891872\ 10^{-3}$	$5.23992\ 10^{-4}$	$6.642\ 10^{-5}$	$-4.26633\ 10^{-4}$
a_5	$-9.211712\ 10^{-5}$	$-9.11628\ 10^{-6}$	$-4.2772\ 10^{-6}$	$9.751\ 10^{-7}$
a_6	$4.415371\ 10^{-7}$	$5.16025\ 10^{-8}$	$4.3691\ 10^{-8}$	$1.39726\ 10^{-8}$

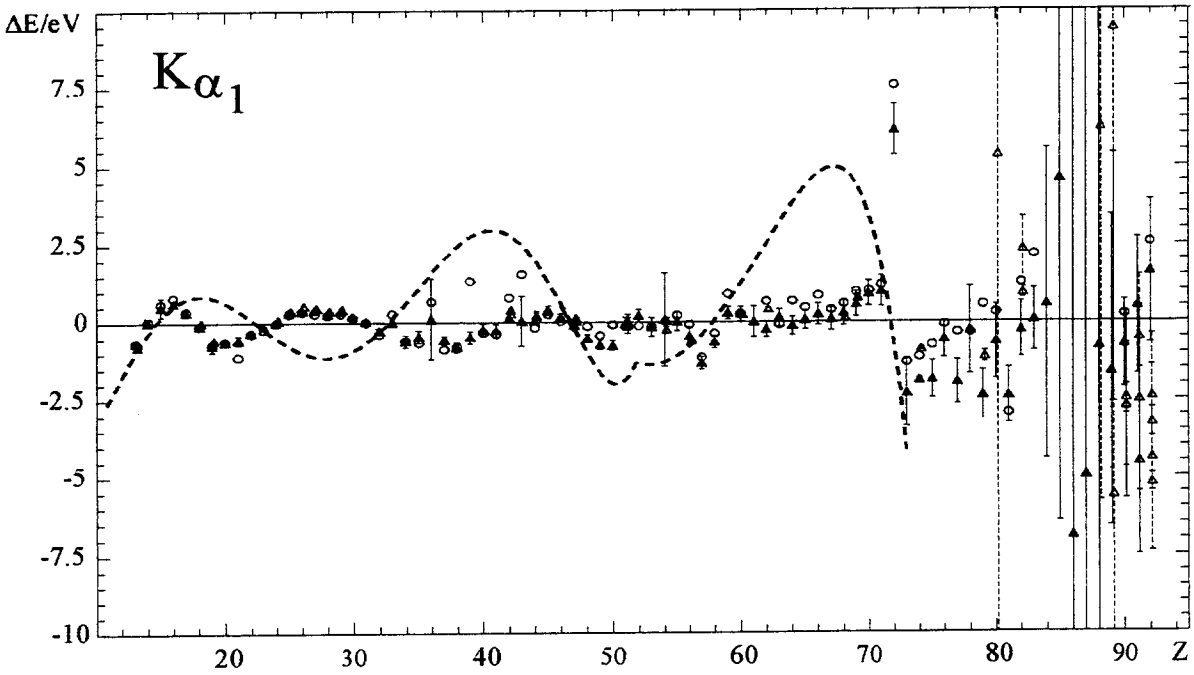

Fig. 1: Differences between experimental $K_{\alpha 1}$ x-ray energies (▲ - [1], ○ - [2], Δ - [6-13]) and values calculated with Eq. (1) plotted versus the atomic number. The differences between an expression published by Norrish and Tao [5] and the present one are depicted by a dashed line.

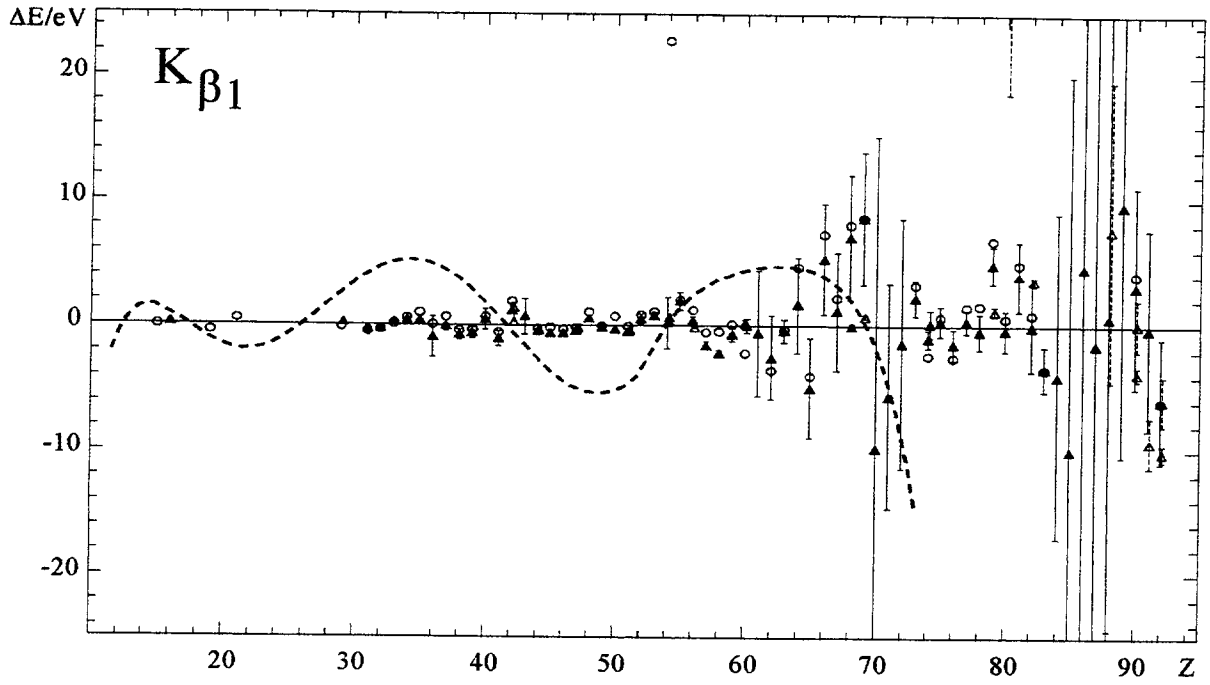

Fig. 2: The same as in Fig. 1 for the $K_{\beta 1}$ transitions.

References

[1] J.A. Bearden, Reviews of Modern Physics 39 (1967) 78.
[2] Y. Cauchois, C. Senemaud, International Tables of Selected Constants, Vol.18, 1978.
[3] Handbook of Chemistry and Physics, 68th edition, ed. by R.C. Weast, CRC Press, Boca Raton, FL, 1987-1988.
[4] G. Zschornack, Atomdaten für die Röntgenspektralanalyse, Springer Verlag, Berlin, 1989.
[5] K. Norrish, G.Y. Tao, X-Ray Spectrometry 22 (1993) 410.
[6] O. Beckman, Physical Review 109 (1958) 1590.
[7] M. Fritsch, Ph.D. Thesis, Friedrich-Schiller-Universität Jena, 1998.
[8] P. Hungerford, H.H. Schmidt, P. Brissot, G. Barreau, H.G. Börner, Z. Naturforsch. 36A (1981) 919.
[9] E.G. Kessler Jr., R.D. Deslattes, W. Schwitz, L. Jacobs, O. Renner, Physical Review A26 (1982) 2696.
[10] M.O. Krause, C.W. Nestor, Jr, Physica Scripta 16 (1977) 285.
[11] T. Mooney, E. Lindroth, P. Indelicato, E.G. Kessler, Jr., R.D. Deslattes, Physical Review A45 (1992) 1531.
[12] M. Polasik, Physical Review A52 (1995) 227.
[13] G. Barreau, H.G. Börner, T.V. Egidy, R.W. Hoff, Zeitschrift für Physik A308 (1982) 209.
[14] M. Deutsch, G. Hölzer, J. Hartwig, J. Wolf, M. Fritsch, E. Förster; Physical Review A51 (1995) 283.

ABTEILUNG NUKLEARCHEMIE, UNIVERSITÄT ZU KÖLN, AND ZENTRUM FÜR STRAHLENSCHUTZ UND RADIOÖKOLOGIE, UNIVERSITÄT HANNOVER

1. Cross Section Measurements for the Production of Residual Nuclei by Medium-Energy Nucleons

M. Gloris[1], S. Neumann[1], I. Leya[1], R. Michel[1], C. Schnabel[1,7], F. Sudbrock[2], U. Herpers[2], O. Jonsson[3], P. Malmborg[3], B. Holmqvist[4], H. Condé[5], P.W. Kubik[6], M. Suter[7], E. Gilabert[8], B. Lavielle[8]

Cross sections for the production of residual nuclei induced by medium-energy protons and neutrons are of interest in a variety of fields. In general, in each application calculations are needed for the activation of matter, e.g. of structural materials in accelerator or space technology. However, since theoretical modeling of the underlying nuclear reactions reveals severe discrepancies in comparison with experimental data [1], measurements are still inevitable if applications demand accurate data. But despite the progress being made in measuring mainly proton-induced production cross sections in the last years (see e.g. [2]) there still exist gaps in the coverage of important projectiles, target elements and product nuclides.

During the last year we continued our efforts to improve this situation. Due to the limited space of this report we will give here only short summaries about the status of our different efforts, with some emphasis on neutron-induced reactions and on the proton-induced reactions in heavy elements. A more detailed overview may be obtained from our contributions to the recent „Nuclear Data for Science and Technology" conference [3-9].

---

[1] Zentrum für Strahlenschutz und Radioökologie, Universität Hannover, Germany
[2] Abteilung Nuklearchemie, Universität zu Köln, Germany
[3] The Svedberg Laboratory, University of Uppsala, Sweden
[4] Department of Neutron Research at Studsvik, University of Uppsala, Sweden
[5] Department of Neutron Research, University of Uppsala, Sweden
[6] Paul Scherrer Institute c/o Institut für Teilchenphysik, ETH Hönggerberg, Zürich, Switzerland
[7] Institut für Teilchenphysik, ETH Hönggerberg, Zürich, Switzerland
[8] Centre d'Etudes Nucléaires de Bordeaux-Gradignan, France

1.1 Neutron-Induced Reactions

Neutron-induced reactions are of special interest in modeling the residual nuclei production in thick targets. If such a target is exposed to energetic projectiles, as e.g. extraterrestrial matter to cosmic radiation, neutrons are produced as secondary particles with energies which are only limited by the primary particles energy. Thus, they contribute to nuclide production in thick targets. But neutron-induced production cross sections above 14 MeV are scarce since there exist just a few facilities which are capable of delivering quasi-monoenergetic medium-energy neutron beams with sufficient flux densities for activation experiments.

A first approach to overcome this situation has been made with the work of Leya [4,10]. By folding experimental thin-target cross sections for the proton-induced production of residual nuclides with calculated proton spectra the proton-related parts of measured production rates of several nuclides in five thick-targets irradiated with protons were calculated. In most cases the assumption holds that differences between the calculated and measured production rates may be attributed to neutron-induced effects. So, it was possible to extract neutron-induced cross sections by deconvolution using an energy-dependent least squares adjustment procedure. This resulted in the establishment of a set of neutron excitation functions for about 500 target/product combinations from their thresholds up to 1.6 GeV with target elements from carbon to lanthanum and via γ-spectrometry detectable nuclides with half-lives between ten hours and thirty years [4,10].

However, since this method is an indirect one with obvious limitations, direct measurements of the neutron-induced residual nuclei production are indispensable. Such investigations were also carried out with a newly installed facility at the The Svedberg Laboratory (TSL)/Uppsala (Sweden). After having demonstrated the feasibility of producing a neutron beam of sufficient flux density for activation experiments we have started to carry out irradiation experiments with neutrons rountinely [6]. Meanwhile three irradiation experiments with ten target elements from carbon to lead were performed with quasi-monoenergetic neutrons of about 75 MeV up to 160 MeV (peak energies). In a fourth experiment absolute and direct measurements of the neutron peak fluence were carried out by means of thin-film breakdown counters [11] in collaboration with the V.G. Khlopin Radium Institute/St. Petersburg (Russia). In combination with the establishment of monitor cross sections for copper and silver using several reactions with different threshold energies this will allow a cross check of the data and result in accurate

deconvolution conditions for the final determination of cross sections. The irradiation experiments at TSL are going on.

In addition to the irradiations at TSL we extended the range of our investigations with neutrons of energies below 70 MeV using the facility of the Université Catholique de Louvain (UCL)/Louvain-la-Neuve (Belgium). Two experiments with quasi-monoenergetic neutron beams were already carried out with peak energies of 33.7 and 46.0 MeV. A third irradiation with 60.6-MeV-neutrons is scheduled for October 1998. Absolute data for the neutron flux density spectrum in the energy range from 3 MeV up to the peak energies were taken by using different measurement techniques [14] from the collaborating group of the Physikalisch-Technische Bundesanstalt/Braunschweig (Germany).

In each case the detection of residual nuclei was performed by using off-line γ-spectrometry requiring careful evaluation of the absolute values of the low induced activities. Data were obtained for nuclides with half-lives between 20 minutes (^{11}C) and five years (^{60}Co). Additionally, the feasibility of the detection of long-lived nuclides, e.g. ^{10}Be ($1.6 \cdot 10^6$ a), from silicon and oxygen by means of accelerator mass spectrometry (AMS) was proved at the ETH/PSI AMS facility in Zurich (Switzerland). Up to now only spectrum-weighted production cross sections can be given since the evaluation of point-wise cross section will not be done before the last irradiation experiment. Only provided with this maximum of information, results with a maximum of accuracy can be obtained within the final deconvolution procedure using least squares methods.

1.2 Proton-Induced Reactions

In contrast to neutron-induced production of residual nuclei the knowledge about the proton-induced one is considerably better. However, even in this case the existing data base needs to be updated for some applications.

This holds, for example, for the modeling of the production of cosmogenic krypton by the proton-dominated cosmic radiation in stony meteoroids and planetary surfaces. Here cross sections for the long-lived and stable Kr-isotopes are essential for the ^{81}Kr-Kr dating method which is known to be one of the most accurate and reliable dating methods. With γ- as well as conventional mass-spectrometric measurements of the proton-induced production of $^{76\text{-}86}$Kr

from Rb, Sr, Y, and Zr in the energy range from some tenths of MeV up to 1.6 GeV [7,12,13] we established a first comprehensive and consistent data base of nearly exclusively new cross sections for model calculations. Moreover, as a by-product more than 360 cross sections for the production of 31 short-lived nuclides were measured by γ-spectrometry prior to mass spectrometry [13].

Further investigations were carried out with respect to the modeling of the production of cosmogenic ^{129}I and ^{41}Ca [8] which have half-lives of $1.57 \cdot 10^7$ and $1.04 \cdot 10^5$ years, respectively. Chemical separation methods were developed for the preparation of samples for the subsequent AMS measurements at the ETH/PSI AMS facility in Zurich (Switzerland). This resulted in the first cross section and production rate measurements of ^{129}I from tellurium and barium in thin and thick targets and allowed for a comparison with model calculations which showed quite a good agreement with the experimental production rates from an artificial meteorite [8].

A step towards a comprehensive data base covering nuclide production in heavy target elements relevant for transmutation techniques has been done with the investigation of proton-induced production of residual nuclei in tantalum, lead and bismuth [3,13]. The evaluation of nearly 1400 very complex (up to 450 peaks) γ-spectra taken off-line after irradiations using stacked-foil-techniques at TSL/Uppsala and the Laboratoire Saturne National (LNS)/Saclay (France) resulted in over 4300 cross sections for about 120 product nuclides with half-lives mainly between ten hours and 520 years. Since proton energies ranged from about 65 MeV up to 2.6 GeV we obtained not only residual nuclei distributions at distinct proton energies but also complete excitation functions which in many cases reach down to the corresponding reaction thresholds.

Although an intensive search of literature was performed, the data found are sparse and originate with only a few exceptions from rather old works. Most of them deal only with nuclides produced in special reaction mechanisms like fission or multifragmentation. In the few cases in which the whole range of residual nuclei is covered these investigations were carried out only for one proton energy. Moreover, a comparison of our cross sections with the data of those works showed that the quality of the latter is very different and that most of our data are completely new. Thus, we have now the worlds largest and most consistent data set with respect to proton-induced production of residual nuclei in heavy elements.

To get an impression of the obtained results Figs. 1-3 give a survey of the cross sections

determined for the target elements tantalum, lead and bismuth for different proton energies in dependence of the mass number of the product nuclides. Several facts become clear in this representation of the data. At low proton energies (Fig. 1) two peaks can be clearly distinguished. The nuclides in the vicinity of the target mass are produced via successive emission of nucleons and nucleon clusters in preequilibrium- and spallation reactions. Since the emission of charged particles is hindered by the high Coulomb barriers of heavy target elements the emission of neutrons is preferred. Therefore nearly exclusively neutron-deficient nuclides were detectable. The increasing width of the spallation peak with increasing proton energy corresponds to the higher number of nucleons which can be emitted if the excitation energies become higher.

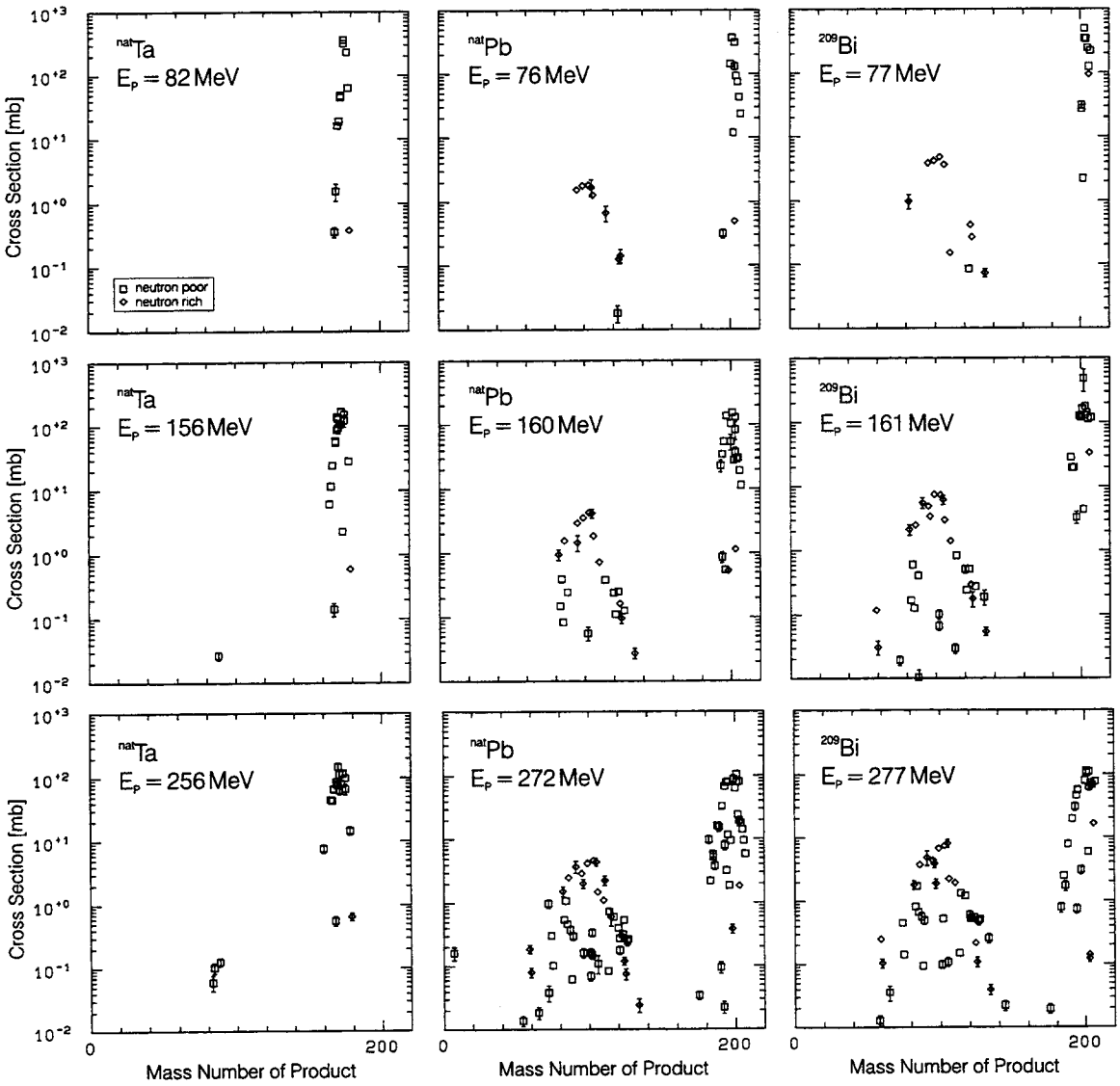

Fig. 1 Measured cross sections in tantalum, lead and bismuth for different proton energies E_P in dependence of the mass number of product nuclides.

In contrast to this reaction mechanism the residual nuclei located at about half of the target mass A are produced via fission reactions. As can be seen the fissionability increases with increasing atomic number Z as well as with increasing proton energies. The first fact is in accordance with the growing fission parameter Z^2/A while the second one is related to the larger number of different fissioning nuclei.

In Fig. 2 these effects become more clear for proton energies between 0.5 and 1 GeV (note that the scale of ordinate has changed). The spallation peak flattens and broadens due to the larger number of emittable nucleons. The fission peak also becomes broader while its height remains at a nearly constant value. Finally, the two regions begin to overlap at about 1 GeV due to the broad range of nuclides produced in spallation reactions.

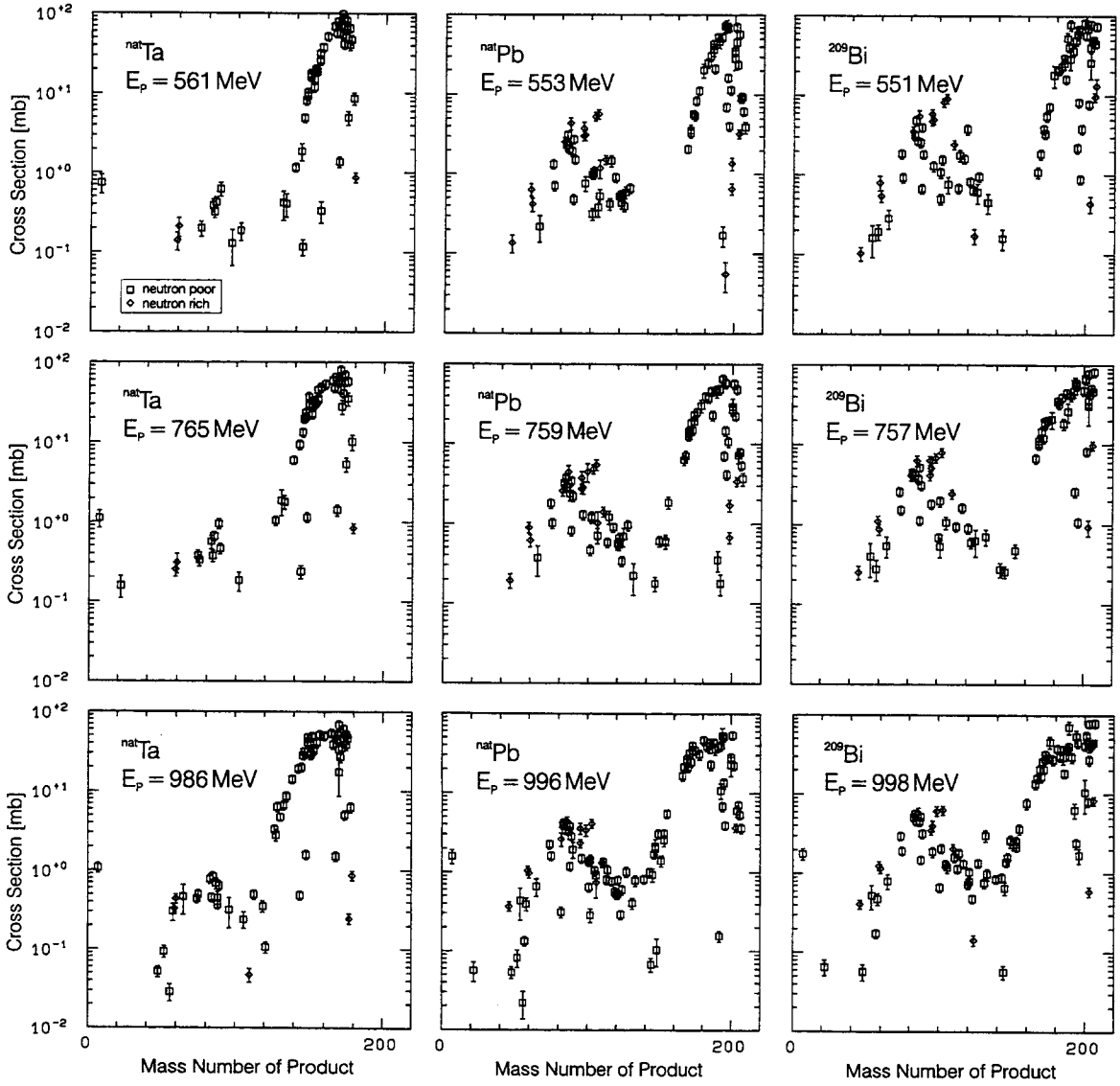

Fig. 2 Measured cross sections in tantauml, lead and bismuth for different proton energies E_P in dependence of the mass number of product nuclides.

In Fig. 3 the results for the highest covered proton energies up to 2.6 GeV are shown. The gap between fission and spallation nuclides is closed by products produced in deep spallation reactions until the influence of fission reactions leaves a signature only in the case of lead and

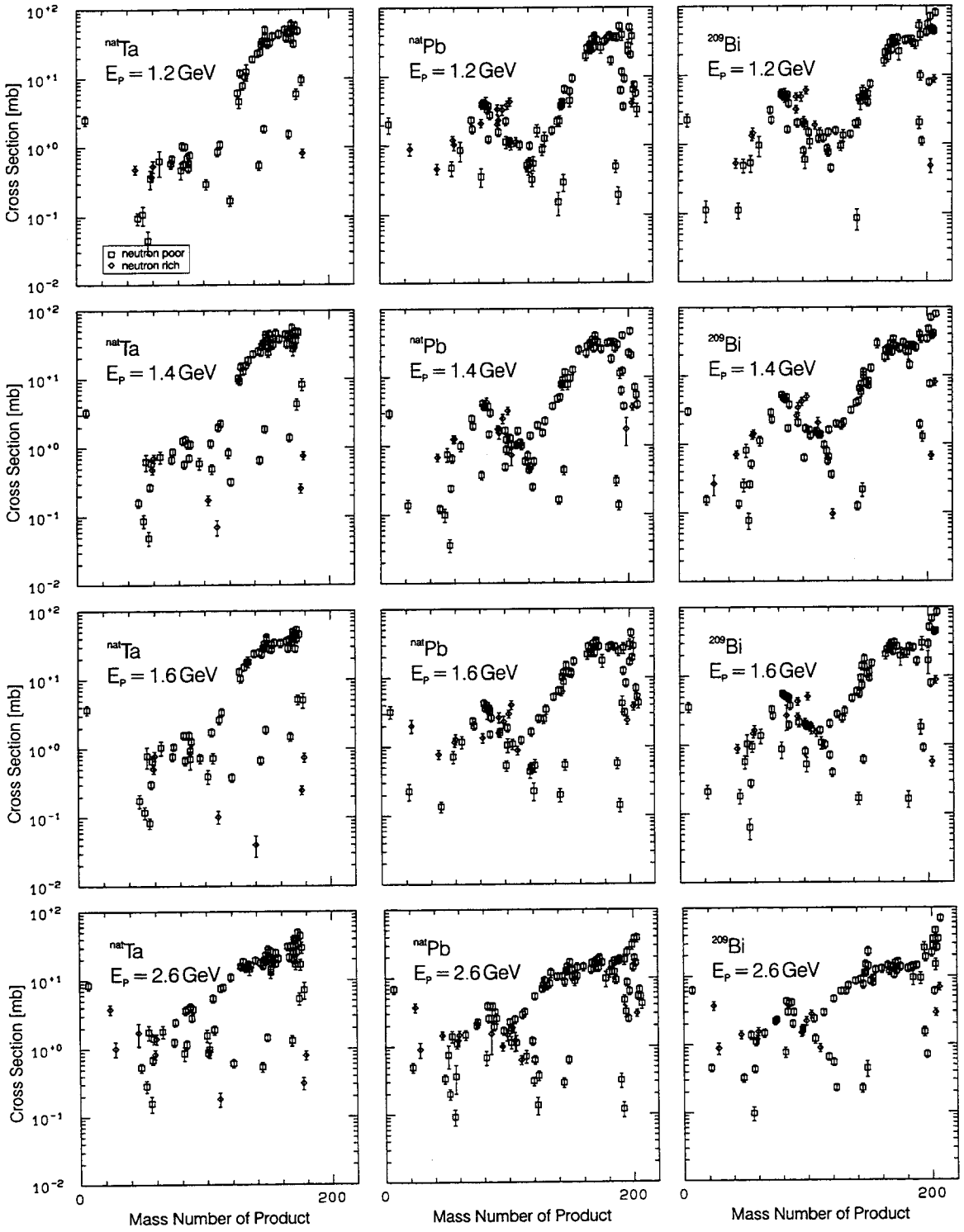

Fig. 3 Measured cross sections in tantalum, lead and bismuth for different proton energies E_P in dependence of the mass number of product nuclides.

bismuth. Additionally, nuclides with very low masses become unambiguosly detectable, thus showing the increasing importance of fragmentation reactions.

With this work [13] a major part of the determination of cross sections for the nuclide production in heavy elements has been done. In spite of that, we performed further irradiation experiments last year at the Paul Scherrer Institute (PSI)/Villigen (Switzerland) to extend and complete our investigations for protons into the low energy range. Several stacks consisting mainly of heavy target elements were irradiated with 72-MeV-protons which were degraded to approximately 35 MeV. The data evaluation will last for some time since the γ-spectrometric measurements are not yet completed. In the next step irradiations with 45-MeV-protons will be performed in order to determine the excitation functions of nuclides with even lower threshold energies.

Production of Long-Lived Residual Nuclides ^{10}Be and ^{36}Cl in Thick-Target Experiments Determined via AMS

F. Sudbrock, U. Herpers, R. Michel, I. Leya, P. W. Kubik, H.-A. Synal, M. Suter

Describing the cosmogenic production of residual nuclides in meteorites requires a detailed comprehension of a variety of factors: energy, flux and composition of the incident particles, size and geometry of the irradiated body and finally the thin-target cross sections of all possibly underlying reactions have to be known precisely [see ref. 15]. In contrast to irradiations where the assumption of an ideal thin-target can be made the nuclide production in thick-targets is governed not only by primary particles but also and often predominantly by secondary particles. This leads to another important difference to thin-target experiments: the particle fluences vary significantly within a thick-target and -what is more- these depth-dependent particle fluxes may show matrix effects, i.e. they in turn depend on the bulk composition of the thick-target.

The production of nuclides in thick-targets can be described with a good accuracy by physical models if all the above mentioned parameters are adequately known. But on the other hand an experimental approach of simulating thick-target irradiations also makes the depth-dependent production rates accessible. Two thick-target experiments were therefore carried out at the

LNS/Saclay (France) with primary proton energies of 1.6 GeV, the first one in 1989 using a gabbro-matrix of 25 cm radius with a chemical composition close to the composition found for stony meteorites and the second one in 1992 with an iron sphere of 10 cm radius as matrix. Details concerning the experimental set-ups may be found in various references [15-19]. The spheres contained sets of high purity thin-target foils which recorded the nuclear reactions induced by primary and secondary particles. The foils were measured exhaustively via γ-spectrometry in Cologne and Hannover before long-lived radionuclides (^{10}Be, ^{26}Al, ^{36}Cl) were separated by radiochemical methods.

The results of both experiments obtained up to now are discussed elsewhere [see ref. 20] so that this contribution wants to focus on a brief discussion of recent results on long-lived nuclides ^{10}Be and ^{36}Cl produced in the target elements calcium, titanium, iron, and nickel which have been measured via AMS at the ETH/PSI AMS facility in Zurich (Switzerland). The order of magnitude and the shape of all depth-profiles for ^{10}Be and ^{36}Cl produced in the iron-sphere is comparable to what was found for the gabbro-sphere which allows to draw the conclusion that matrix effects for these target/product combinations are merely imperceptible. In addition, theoretical analyses have been performed [21] which give in all cases very satisfying results as they reproduce the shape and absolute values reasonably well and they allow to discriminate the influence of primary and secondary particle induced reactions.

In most cases the production of the nuclides under consideration is quite similar [19], i.e. constant over the whole sphere with calcium being a remarkable exception as the production of ^{36}Cl shows a strong increase from surface to center [19]. For this particular case of target-near residual nuclides the secondary neutron induced reactions have to be considered as a predominant production path. A theoretical analysis [21] of the experimental depth-profile for this reaction clearly confirms this hypothesis.

Acknowledgement:

The authors thank the authorities of LNS, PSI, UCL and TSL for the beam-time and the accelerator staffs for their essential cooperation and support. This work was supported partially by the Deutsche Forschungsgemeinschaft, Bonn, the CEC in the Human Capital and Mobility Programme and the Swiss National Science Foundation, Bern.

References

[1] R. Michel, P. Nagel, International Codes and Model Comparison for Intermediate Energy Activation Yields, NSC/DOC(97)-1, NEA/OECD, Paris, 1997.

[2] R. Michel et al., Cross Sections for the Production of Residual Nuclides by Low- and Medium-Energy Protons from the Target Elements C, N, O, Mg, Al, Si, Ca, Ti, Mn, Fe, Co, Ni, Cu, Sr, Y, Zr, Nb, Ba and Au, Nucl. Instr. Meth. Phys. Res. B129 (1997) 153.

[3] M. Gloris R. Michel, F. Sudbrock, U. Herpers, D. Filges, P. Malmborg, B. Holmqvist, H. Condé, Proton-Induced Nuclide Production in Heavy Target Elements at Medium Energies, in: G. Reffo, A. Ventura, C. Grandi (eds.), Proc. Int. Conf. Nuclear Data for Science and Technology, Trieste, 19-24 May 1997, IPS Conf. Proc. 59 Bologna (1997) 1468.

[4] I. Leya, R. Michel, Determination of Neutron Cross Sections for Nuclide Production at Intermediate Energies by Deconvolution of Thick-Target Production Rates, ibid. 1463.

[5] R. Michel et al., A New Experimental Database of Cross Sections for the Production of Residual Nuclides by Proton-Induced Reactions on the Target Elements C, N, O, Mg, Al, Si, Ca, Ti, V, Mn, Fe, Co, Ni, Cu, Sr, Y, Zr, Nb, Ba and Au from Thresholds up to 2.6 Gev, ibid. 1458.

[6] S. Neumann, R. Michel, F. Sudbrock, U. Herpers, P. Malmborg, O. Jonsson, B. Holmqvist, H. Condé, P.W. Kubik, M. Suter, A New Facility at the The Svedberg Laboratory for Activation Experiments with Medium Energy Neutrons, ibid. 379.

[7] S. Neumann, M. Gloris, R. Michel, E. Gilabert, B. Lavielle, Th. Schiekel, U. Herpers, Measurement and Calculation of Proton-Induced Integral Cross Sections of Stable Krypton Isotopes for Energies up to 1.6 GeV on Rb, Sr, and Y, ibid. 1519.

[8] C. Schnabel, P. Gartenmann, J.M. Lopez-Guitierrez, B. Dittrich-Hannen, M. Suter, H.-A. Synal, I. Leya, M. Gloris, R. Michel, F. Sudbrock, U. Herpers, Determination of Proton-Induced Production Cross Sections and Production Rates of ^{129}I and ^{41}Ca, ibid. 1559.

[9] F. Sudbrock, A. Berkle, U. Herpers, U. Neupert, M. Gloris, I. Leya, R. Michel, H.-A. Synal, P.W. Kubik, H.-A. Synal, G. Bonani, M. Suter, et al., Cross Sections for the Proton-Induced Production of the Long-Lived Radionuclides ^{10}Be, ^{14}C and ^{36}Cl Measured via Accelerator Mass Spectrometry, ibid. 1534.

[10] I. Leya, Model Calculations for the Description of the Interaction of Galactic Cosmic Particle Rays with Stony and Iron-Meteorites - Thin Target Irradiations and Thick Target Experiments (translated title), Ph. D. Thesis, University Hanover (1997).

[11] V.P. Eismont, A.I. Obukhov, A.V. Prokofyev, A.N. Smirnov, Relative and absolute neutron-induced fission cross sections of ^{208}Pb, ^{209}Bi, and ^{238}U in the intermediate energy region, Phys. Rev. C53 (1996) 2911.

[12] E. Gilabert, B. Lavielle, S. Neumann, M. Gloris, R. Michel, Th. Schiekel, F. Sudbrock, U. Herpers, Cross Sections for the Proton-Induced Production of Krypton Isotopes from Rb, Sr, Y, and Zr for Energies up to 1600 MeV, to be submitted to Nucl. Instr. Meth. Phys. Res. B (1998).

[13] M. Gloris, Proton-induced Production of Residual Nuclei in Heavy Elements at Medium Energies (translated title), Ph. D. Thesis, University Hanover (1998).

[14] H. Schumacher, H.J. Brede, V. Dangendorf, M. Kuhfuss, J.P. Meulders, W.D. Newhauser, R. Nolte, U.J. Schrewe, Quasi-Monoenergetic Reference Neutron Beams with Energies from 25 MeV to 70 MeV, in: G. Reffo, A. Ventura, C. Grandi (eds.), Proc. Int. Conf. Nuclear Data for Science and Technology, Trieste, 19-24 May 1997, IPS Conf. Proc. 59 Bologna (1997) 1534.

[15] R. Michel, I. Leya, L. Borges, Nucl. Instr. Meth. in Phys. Res. B113 (1996) 434.

[16] R. Rösel, Ph. D. Thesis, University of Cologne (1995).

[17] I. Leya, Ph. D. Thesis, University Hannover (1997).

[18] T. Schiekel, Ph. D. Thesis, University of Cologne (1995).

[19] F. Sudbrock, Ph. D. Thesis, University of Cologne (1998).

[20] I. Leya, et al., to be submitted to Meteoritics and Planetary Science (1998).

[21] I. Leya, priv. comm. (1997).

INSTITUT FÜR KERNCHEMIE
UNIVERSITÄT MAINZ

Odd-Even Effects in the Fission of Odd-Z Nuclides

M. Davi[1], H. O. Denschlag[1], H. R. Faust[2], F. Gönnenwein[3], S. Oberstedt[2]
I. Tsekhanovitch[1,4], M. Wöstheinrich[3]

Odd-even effects in the yield distribution of fission fragments are normally understood as a preferential formation of fission products with even atomic number (Z) (or even neutron number, N) relative to odd fission products. Odd-even effects of this sort have been observed in nearly all low energy fission processes of even Z fissioning nuclei in the mass range of the compound nuclei from A_F=230 to A_F=250. They have been interpreted as a consequence of the preservation of nuclear pairing (superfluidity) in the fissioning nuclei on the way from saddle point to scission and, hence, of an adiabatic character of the fission process leading to low internal excitation energy at scission.

Some time ago, some of us [1, 2] found evidence for a proton odd-even effect among the very light fission products in the fission of the odd-Z compound nucleus ^{243}Am* (Z=95). An odd-even effect in an odd-Z system is different from the effect discussed above:

1.) Due to the fact that in 99.8 % of the fission events no third charged particle is emitted, the total yield of even-Z and odd-Z fragments is equal by definition (within 99.8%) and a preferential formation of **even light** fission fragments must be accompanied by a preferential formation of **odd heavy** fragments.

2.) The reasoning given above of a preservation of nuclear pairing is not applicable to a system that has an unpaired nucleon already in its ground state. Such a system is not expected to preserve superfluidity on the way from saddle point to scission and hence is likely to pick up a higher excitation energy than a fully paired system.

Recently, we could extend the previous measurements in the fission of ^{243}Am* to more asymmetric mass splits. In addition, measurements were performed in another odd-Z fissile nucleus (^{239}Np, Z=93). As reported before [1,2], the measurements were performed at the mass separator Lohengrin of the Institut Laue-Langevin using ionisation chambers with a split anode for the Z-identification of the mass separated fission fragments. For the evaluation of the odd-even effects as a function of the nuclear charge of the fragments, the method of Tracy et al. [3] was used. The method uses four consecutive nuclear charges (Z_0 to Z_3) to provide an odd-even effect for a mean nuclear charge $Z_m=Z_0+1.5$.

The results confirm fully our previous measurements. Figure 1 shows the odd even effects observed in the two fission reactions as a function of the mean atomic number of the light fragment (Z_m). Whereas both fission reactions show no odd-even effects in the regions of the most frequent mass splits (nuclear charge splits; Z_L>37) (in Fig. 1 only shown for ^{239}Np), odd-even effects are observed for Z_L<36. These odd-even effects show an increase with decreasing Z_m, i.e. with increasing mass asymmetry of the fission

---

[1]Institut für Kernchemie, Universität Mainz, D-55099 Mainz, Germany
[2]Institut Laue-Langevin, F-38042 Grenoble, Cedex, France
[3]Physikalisches Institut, Universität Tübingen, D-72076 Tübingen, Germany
[4]Radiation Physics and Chemistry Problems Institute, 220109 Minsk, Belarus

fragments. The effects are larger for $^{239}Np^*$ than for $^{243}Am^*$ and, therefore seem to decrease with increasing fissility parameter (Z^2/A).

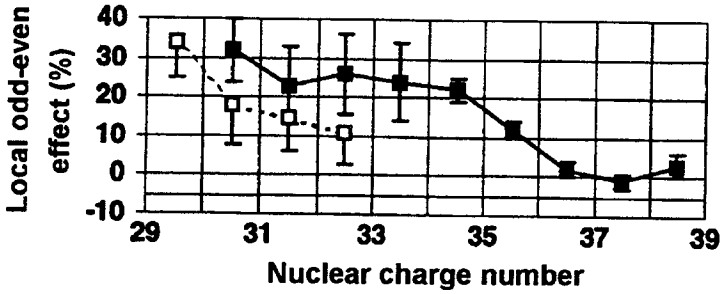

Figure 1 Local odd-even effects (%) in the fission of $^{239}Np^*$ (upper curve) and $^{243}Am^*$ (lower curve). For clarity of display the error margins in the lower curve are given in the downward direction only. They are to be understood as symmetric around the data points.

Recently, the observations made by our group in the thermal neutron induced fission has been confirmed also for fission in inverse kinematics [4].

These findings shed a new light on the understanding of the odd-even effect and support our previous proposition [1,2] that statistical processes may play a role for the question on whether the unpaired nucleon will end up with the light or heavy fragment. In this context the recent idea [4] seems very interesting, that the probability to capture the (least bound) unpaired proton depends on the phase space available in the forming fragments and that this phase space is proportional to the number of nucleons in the fragment. A more detailed presentation of this work can be found in Ref. [5]

References

[1] P. Stumpf, U. Güttler, H.O. Denschlag, H.R. Faust: Odd-even Effects in the Reaction $^{241}Am(2n,f)$; in: S. Cierjacks (Ed.), Progress Report on Nuclear Data Research in the Federal Republic of Germany, Report No.: NEANDC(E)-322-U-Vol. V/INDC(Ger)-36/LN+Special/KfK 4953.

[2] P. Stumpf, U. Güttler, H.O. Denschlag, H.R. Faust:, Odd-Even Effects in the Reaction $^{241}Am(2n,f)$, in Nuclear Data for Science and Technology, S.M. Qaim, Editor, 1992, Springer, Berlin. p. 145.

[3] B. L. Tracy, J. Chaumont, R. Klapisch, J. M. Nitschke, A. M. Poskanzer, E. Roeckl, C. Thibault; Phys. Rev. C5, 222 (1972)

[4] S. Steinhäuser, J. Benlliure, C. Böckstiegel, H.-G. Clerc, A. Heinz, A. Grewe, M. de Jong, A.R. Junghans, J. Müller, M. Pfützner, K.H. Schmidt: Odd-even effects observed in the fission of nuclei with unpaired protons; Nucl. Phys. A634, 89 (1998).

[5] M. Davi, H. O. Denschlag, H. R. Faust, F. Gönnenwein, S. Oberstedt, I. Tsekhanovitch, M. Wöstheinrich: Odd-Even Effects in the Fission of Odd-Z Nuclides, to appear in Proceedings 2nd Int. Workshop on Nuclear Fission and Fission-Product Spectroscopy, Seyssins, France (1998), American Institute of Physics, in press.

INSTITUT FÜR KERNCHEMIE
PHILIPPS-UNIVERSITÄT MARBURG

^{257}Fm: Direct Determination of Partial Neutron Multiplicities in Correlation with Fission-Fragment Mass and Energy

K. Siemon, R.A. Esterlund, J. van Aarle, W. Westmeier and P. Patzelt

Using a large Gd-doped liquid-scintillator tank (neutron sphere), the *partial* neutron multiplicities for ^{257}Fm have been measured *directly* as a function of fission-fragment mass and energy. This assignment of neutrons to a specific fission fragment was achieved *via* separate counter electronics for the two divided halves of the neutron sphere. The fission-fragment detectors are placed in such a manner that they preferentially select those events whose vectors point well into the semi-spheres, thus achieving the greatest efficiency for neutrons from a given fission fragment to be registered in their corresponding semi-sphere and *vice-versa*. Moreover, these new data have been corrected so as to eliminate non-full-energy events.

A detailed description of the neutron sphere detector used for the measurements is given elsewhere [1-3]. In many previous works [1, 4-6] where neutron multiplicities are indirectly assayed with a high-efficiency liquid-scintillation counter, the procedure suffers from two disadvantages: 1) if one or more of the γ-rays associated with neutron capture in one semi-sphere enters the other semi-sphere and is detected there, coincident registration of one neutron in each semi-sphere will occur (cross-talk); 2) if the velocity vector of a neutron is larger than and oriented opposite to the corresponding fission-fragment velocity vector, then

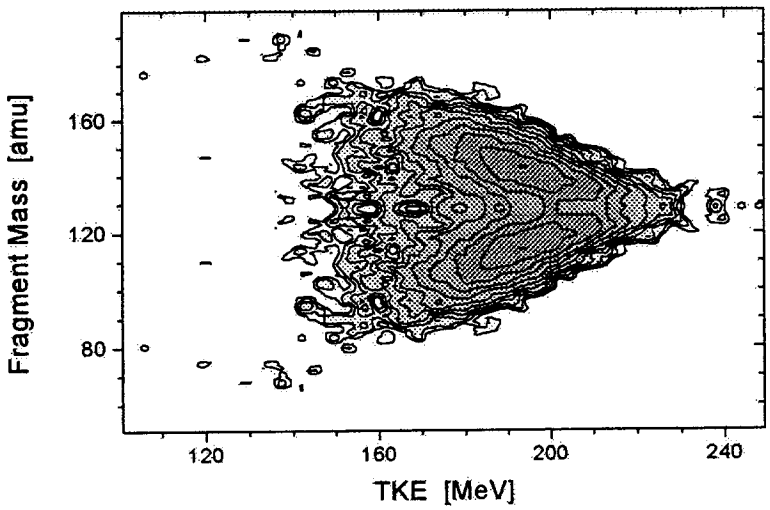

Fig. 1 Fission-yield distributions for the spontaneous fission of ^{257}Fm as a function of the TKE and fragment mass, for the experimental total neutron multiplicity $\nu_t = 4$.

the neutron corresponding to one semi-sphere will in fact be registered in the other semi-sphere, thus being correlated with the wrong fission fragment. In the present experiment, events with γ-ray cross-talk (point 1 above) have been correctly sorted by using a special fast-logic veto circuit.

We now present a very small sampling of the extensive data base which we have measured for this system. Fig. 1 depicts fission-yield distributions for the spontaneous fission of ^{257}Fm as a function of the TKE and fragment mass, for the experimental total neutron multiplicity $\nu_t = 4$. The maximum in this contour plot corresponds to 13.6 events, and the total number of events measured in this case is 6880. Similar contour plots are available for total neutron multiplicities $\nu_t = 0$ to 3 and 5 to 9.

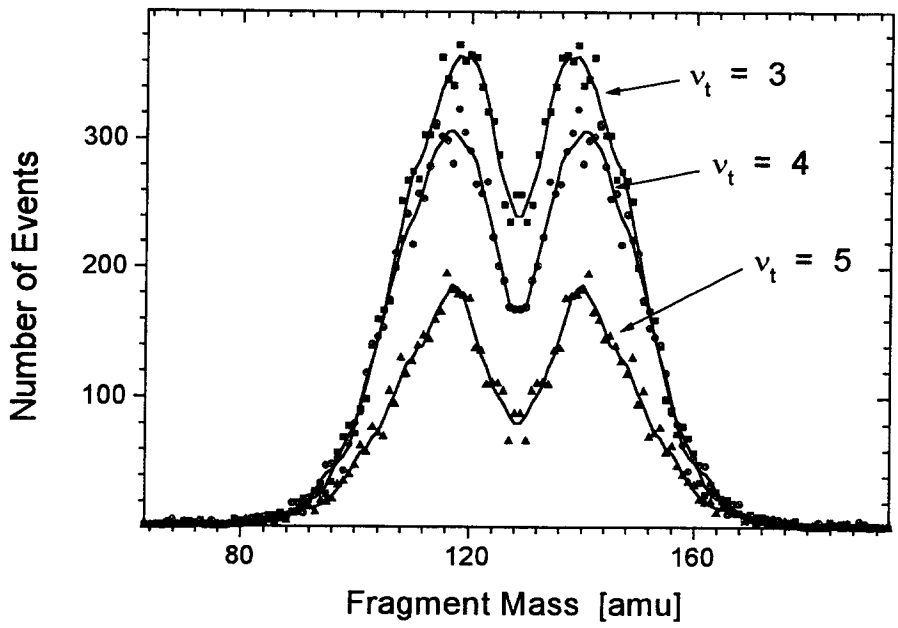

Fig. 2 Fission-fragment mass distributions depicting the positions and widths corresponding to experimental total neutron multiplicities ν_t = 3, 4, 5.

Fig. 2 displays fission-fragment mass distributions corresponding to experimental total neutron multiplicities ν_t = 3, 4, 5. The light-fragment masses corresponding to these total neutron multiplicities are A = 114.73 ± 1.28, 113.71 ± 1.38 and 113.50 ± 1.86 amu, respectively. The widths expressed as standard deviations σ are 8.88 ± 1.37, 9.22 ± 1.49 and 9.08 ± 1.65, and the total numbers of events measured in each case are 8021, 6880 and 3750.

Finally, Fig. 3 displays the distribution of the mean, efficiency-corrected, partial-neutron multiplicities as a function of the TKE and mass of the fission fragments from the spontaneous fission of ^{257}Fm. These data originate from the measurement of more than 30,000 fission events. Details will be presented in a forthcoming paper.

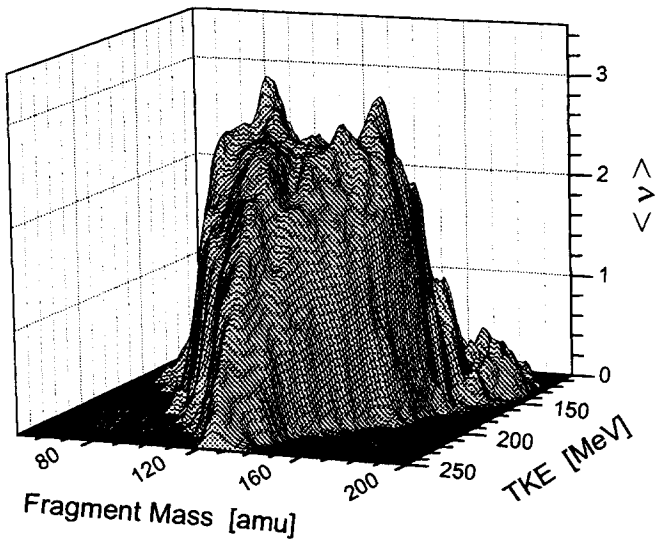

Fig. 3 The mean, efficiency-corrected, partial-neutron multiplicities as a function of the TKE and mass of the fission fragments from the spontaneous fission of ^{257}Fm.

References

[1] J. van Aarle, W. Westmeier, R.A. Esterlund and P. Patzelt: ^{252}Cf: Neutron Multiplicities in Correlation with Fission-Fragment Mass and Energy, Nucl. Phys. A578 (1994) 77, as well as in: Progress Report on Nuclear Data Research in the Federal Republic of Germany, NEA/NSC/DOC(94)21, ed. S.M. Qaim (Aug. 1994) 43

[2] J.F. Wild, J. van Aarle, W. Westmeier, R.W. Lougheed, E.K. Hulet, K.J. Moody, R.J. Dougan, E.-A. Koop, R.E. Glaser, R. Brandt and P. Patzelt: Prompt Neutron Emission from the Spontaneous Fission of ^{260}Md, Phys. Rev. C41 (1990) 640

[3] J. van Aarle: Untersuchungen zur Spontanspaltung von ^{260}Md und ^{252}Cf (Doctoral thesis, Universität Marburg, 1992, unpublished)

[4] C. Budtz-Jørgensen and H.-H. Knitter: Simultaneous Investigation of Fission Fragments and Neutrons in ^{252}Cf (SF), Nucl. Phys. A490 (1988) 307

[5] See, *e.g.*, I. Düring, U. Jahnke and H. Märten: Fragment-Neutron and Neutron-Neutron Correlations in ^{252}Cf Spontaneous Fission, Progress Report on Nuclear Data Research in the Federal Republic of Germany, NEA/NSC/DOC(94)21, ed. S.M. Qaim (Aug. 1994) 19

[6] See, *e.g.*, I. Düring, M. Adler, H. Märten, A. Ruben, B. Cramer and U. Jahnke: Multi-fold Correlations Between ^{252}Cf (sf) Fragments and Fission-Neutron γ-Rays, in Proceedings of the International Workshop on High-Resolution Spectroscopy of Fission Fragments, Neutrons and γ-Rays, FZR 93 - 08, eds. H. Märten and K.D. Schilling (Mar. 1993) 103

**FAKULTÄT FÜR PHYSIK DER
TECHNISCHEN UNIVERSITÄT MÜNCHEN
REAKTORSTATION GARCHING**

Total Cross Section Measurements with Cold Neutrons on Solid and Powder Samples and on Hydrogen Containing Compounds*

K. Knopf, W. Waschkowski

Transmission measurements with cold neutrons of mean energy 0.57 meV on solid and powder samples were performed to deduce the inelastic scattering cross section σ_{inel} and the absorption cross section σ_γ for 43 chemical elements and 27 of their isotopes. The Debye-temperature Θ_D could be deduced from the measurements.

From similar experiments on water, alcohol and carbon hydrogen compounds the proton scattering cross section for cold neutrons was determined.

*J. Neutron Research. 5, (1997) 147-165

Evaluation of Neutron Fundamental Parameters from the Total Cross Section Data*

A. Aleksejevs[1], S. Barkanova[1], T. Krasta[1], P. Prokofjevs[1], J. Tambergs[1], W. Waschkowski, G.S. Samosvat[2]

Using experimental data from neutron transmission measurements on enriched $^{206,207,208}Pb$, natural Pb and Bi targets, the potential scattering radii R' and the electric polarizability of the neutron α_n were determined by general least squares fit at fixed neutron-electron bound scattering length values: $b_{ne} = -1.32 \cdot 10^{-3}$ fm (Garching) and $b_{ne} = -1.59 \cdot 10^{-3}$ fm (Dubna). The evaluations were performed in two versions: (1) The potential scattering radii R' were taken as fitted parameters; (2) R' values were deduced from optical model calculations. The obtained potential scattering radii values are in the range of 9.0 to 10.0 fm. The electric polarizability of the neutron in the first version resulted in $\alpha_n = +(0.12 \pm 0.44) \cdot 10^{-3}$ fm^3 with the Garching b_{ne} value and $\alpha_n = -(0.97 \pm 0.44) \cdot 10^{-3}$ fm^3 with the Dubna b_{ne} value, but in the second calculation version in $\alpha_n = -(0.14 \pm 0.37) \cdot 10^{-3}$ fm^3 with both b_{ne} values. On the basis of obtained results we give preference to the Garching b_{ne} value.

*Physica Scripta 56, (1997) 20-25

[1] Nuclear Research Center, LV-2169 Salaspils-1, Latvia
[2] Frank Laboratory of Neutron Physics, JINR, 14980 Dubna, Moscow region, Russia

Interaction of Slow Neutrons with Natural Terbium, Holmium and Erbium and its Isotopes*

K. Knopf, W. Waschkowski

Coherent neutron scattering lengths and total cross sections have been measured on samples of natural Tb, Ho and Er and on isotopically enriched Er-compounds. From the experiment the following data were obtained:

- the coherent scattering lengths (in fm) of the bound atoms
  ^{159}Tb(7.34 ± 0.02), ^{165}Ho(8.44 ± 0.03), ^{ord}Er(7.79 ± 0.02),
  ^{162}Er(9.01 ± 0.11), ^{164}Er(7.95 ± 0.14), ^{166}Er(10.51 ± 0.19),
  ^{167}Er(3.06 ± 0.05), ^{168}Er(7.43 ± 0.08), and ^{170}Er(9.61 ± 0.06);
- the thermal absorption cross sections (in b)
  ^{141}Pr(12.7 ± 0.6), ^{nat}Nd(58 ± 1), ^{159}Tb(30 ± 2), ^{165}Ho(65 ± 2);
  ^{nat}Er(145 ± 2), ^{166}Er(18 ± 2), ^{167}Er(568 ± 9), ^{168}Er(2.3 ± 0.3), and ^{170}Er(15 ± 1).

In combination with the resonance parameters, the measured coherent scattering lengths allowed the determination of potential scattering radii R' which are of particular interest for the optical model theory.

*Z. Phys. A 357, (1997) 297-302

PHYSIKALISCH-TECHNISCHE BUNDESANSTALT BRAUNSCHWEIG

1. Angular Distributions of Elastic Neutron Scattering on ^{51}V

D. Schmidt, W. Mannhart

The present experiment covers the neutron energy range between 8.0 and 14.4 MeV. Below 14 MeV experimental scattering data are scarce due to the lack of a real monoenergetic neutron source. In the case of ^{51}V, with an isotopic abundance of 99.75%, no results of previous measurements were available between 11 and 14 MeV, and below 11 MeV other experiments were performed only at a few neutron energies.

The angular distributions, as given in Fig. 1, show a pronounced structure with large gradients $d\sigma/d\Theta$ and deep minima. To reproduce these details, a well-established scale of scattering angles is mandatory. It was found that the geometric angle defined between the deuteron beam axis and the axis between the centres of the sample and the neutron detector is not a trustworthy quantity. Due to unknown variations in the beam axis and due to the finite geometry of target, sample and detector, the effective scattering angle (mean value of the angle density distribution) deviates from the geometric one. To determine the effective scattering angle we use the neutron scattering on hydrogen at forward angles which kinematically is quite sensitive to the angle position. This method, combined with a realistic Monte Carlo simulation of the finite scattering geometry of our experiment, is used to adjust the scattering angle. Typical deviations between the effective and the geometric angle are of the order of 1 deg.

Our experiment covers the angular range between 12.5 and 160 deg with data taken at 30 to 40 different angles. Based on an MC simulation of the complete angular distribution with iterative adjustment to the experimental data, corrections for finite geometry, flux attenuation and multiple scattering in the sample were calculated. The procedure resulted in small uncertainties of the measured data which are necessary for a realistc extrapolation of the data to the uncovered ranges with a fit of Legendre polynomials to the data.

The measured angular distributions are shown in Fig. 1. The uncertainties of the individual data points vary between 2.6% and 7.8%, with an unweighted mean of (4.1 ± 1.0) %. The typical uncertainties of the angle-integrated cross sections derived from these data are of the order of 2.5%.

2. Double Differential Neutron Emission Cross Sections of Elemental Chromium for Neutron Energies between 8 and 15 MeV

D. Schmidt, W. Mannhart

Double-differential neutron cross sections of elemental chromium were determined at 10 neutron energies between 7.95 and 14.76 MeV. The analysis is complicated by the breakup neutron contamination (below about 8 MeV neutron energy) of the D(d,n) neutron source

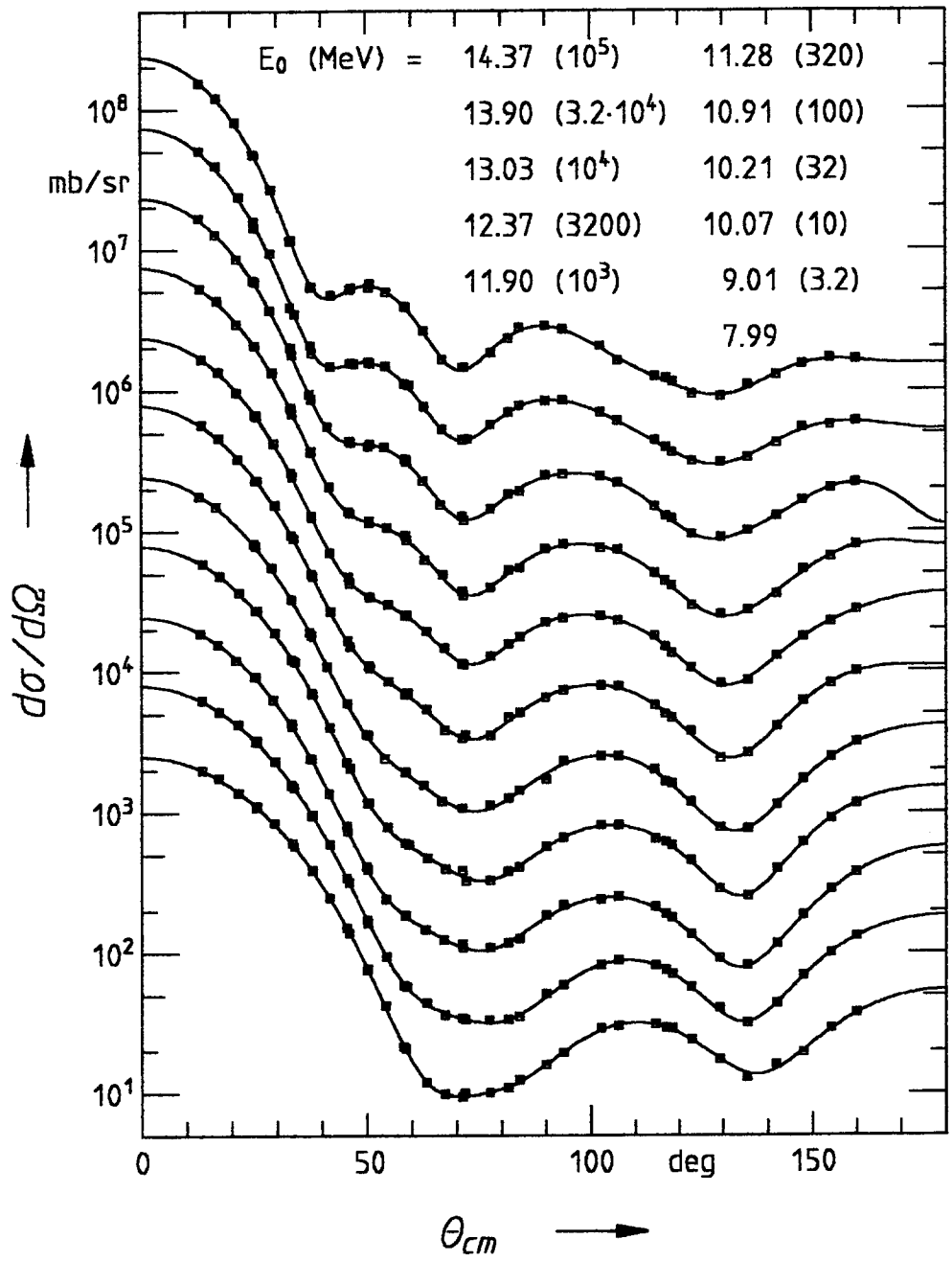

Fig. 1 Angular distributions of elastic neutron scattering on ^{51}V. The neutron energy increases from the bottom to the top of the figure. The values given in parentheses are offset factors.

used. The scattering components of breakup neutrons were calculated with a Monte Carlo simulation of the scattering geometry and subtracted from the measured TOF spectra as briefly outlined elsewhere [1,2].

The database of the MC simulation was derived from the ENDF/B-VI evaluation and combined with recent experimental data of elastic neutron scattering measured at ANL below 10 MeV [3]. Often the evaluated elastic and inelastic data deviate significantly from the measured ones [4]. To circumvent this deficiency, additional measurements were carried out at

14.1 MeV with the ^{4}He(d,np) reaction, a pure breakup neutron source, and used to adjust the cross section data. In a first step, only the inelastic data were adjusted in five iterative steps. The remaining differences of less than 10% between measurement and calculation were then reduced by adjusting all data. We learned from the present analysis that elastic and inelastic cross section data must be adjusted independently and that additional measurements at lower energies with the ^{4}He(d,np) breakup neutron source are highly desirable in future experiments.

As an example of the results obtained, Fig. 2 shows the neutron emission spectrum at 9.80 MeV incident neutron energy compared with the ENDF/B-VI evaluation. The evaluation comprises the inelastic scattering to discrete levels and to the continuum of all four chromium isotopes. Between 2 MeV and 4 MeV, the ENDF cross sections are smaller by about 20% than our data and between 4 MeV and 7 MeV they exceed our data by about 26%. These deviations cannot be explained by inconsistencies in our breakup correction.

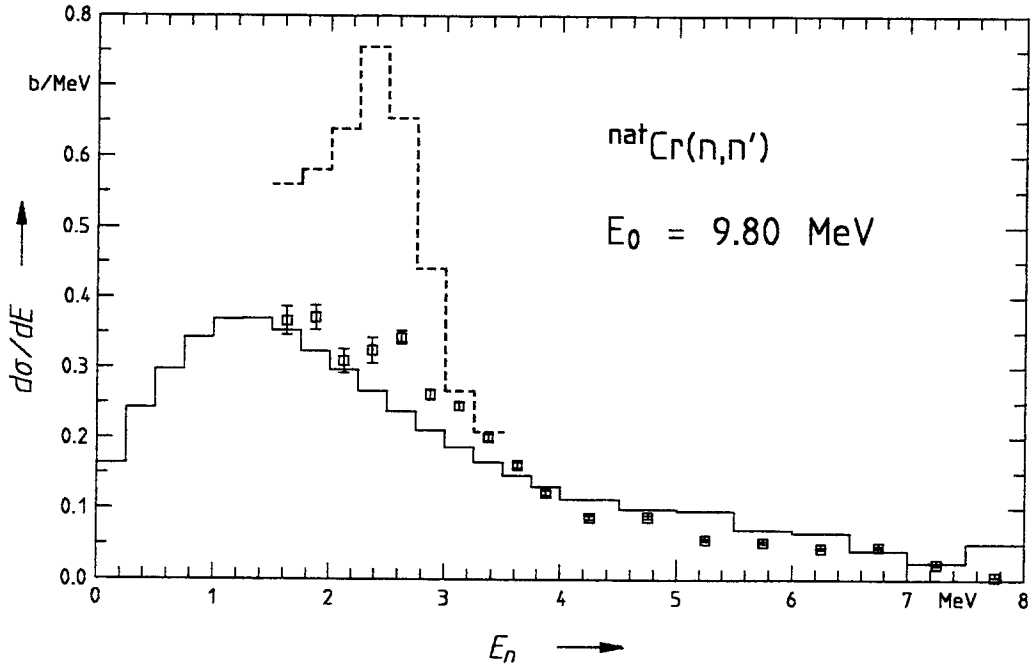

Fig. 2 Neutron emission spectrum of elemental chromium at 9.80 MeV incident neutron energy. The present data are given as squares with error bars. The histogram (dashed line) shows the data before applying the breakup correction, and the histogram with the full line represents the ENDF/B-VI evaluation.

3. Measurement of the ^{51}V(n,p)^{51}Ti Cross Section between 7.9 and 14.4 MeV

W. Mannhart, D. Schmidt, D.L. Smith*

Vanadium is a potential candidate as a low-activation structural material in the design of a future fusion reactor. At 15 neutron energies between 7.89 and 14.45 MeV, cross section data of the ^{51}V(n,p)^{51}Ti reaction were measured. Neutrons were produced through the D(d,n)^{3}He

*Argonne National Laboratory, Argonne, USA

reaction, with appropriate corrections for parasitic neutrons stemming from the deuterium breakup reactions. The neutron fluence was monitored with a low-mass ^{238}U fission chamber. All data are thus based on the $^{238}U(n,f)$ cross section taken from the ENDF/B-VI evaluation. The radioactivity of the 5.76 min decay of ^{51}Ti was measured with a 300 cm^3 HPGe detector calibrated in the photopeak efficiency with an uncertainty of 1.5%. Corrections were applied for finite geometry, self-absorption and coincidence summing effects.

Our measurements fill the data gap of this reaction between 9.3 and 13.4 MeV and are shown in Fig. 3. The excitation function measured in the present experiment shows slight structures which are averaged in the ENDF/B-VI evaluation. Between 12 and 13 MeV, our data exceed the ENDF/B-VI evaluation by about 7%. Below 9.3 MeV, our data show fair agreement with the previous experiment of Smith et al. [5]. Above 13.2 MeV, our data fully confirm the experiment of Ikeda et al. [6] up to 14.4 MeV.

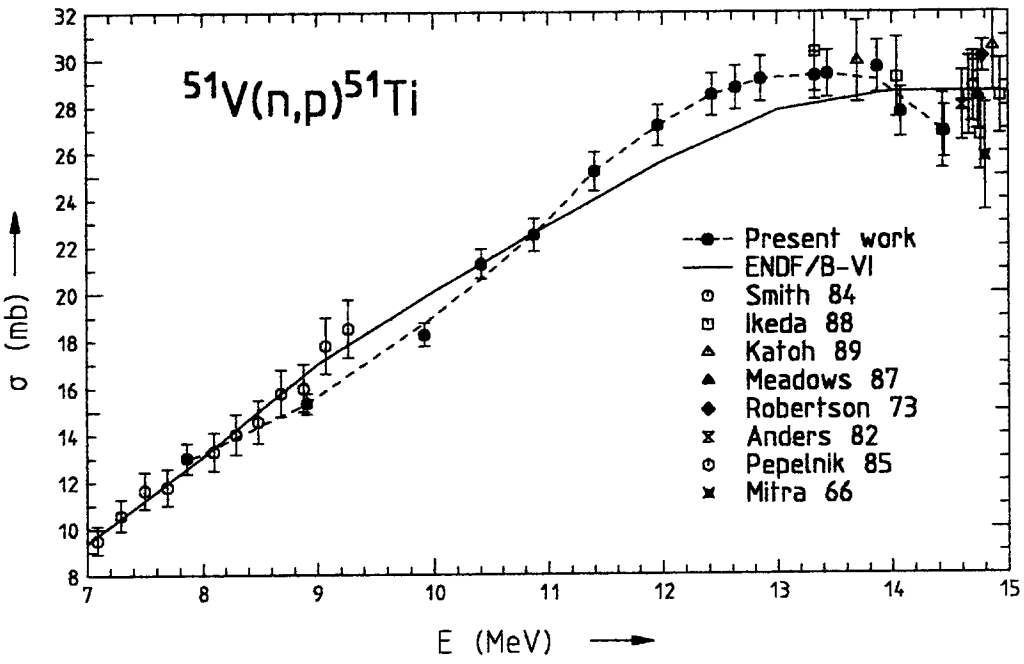

Fig. 3 Excitation function of the $^{51}V(n,p)^{51}Ti$ reaction

4. Measurement of the $^{51}V(n,\alpha)^{48}Sc$ Cross Section between 7.9 and 14.4 MeV

W. Mannhart, D. Schmidt, D.L. Smith*

Besides the short-lived $^{51}V(n,p)^{51}Ti$ reaction, the activation reaction $^{51}V(n,\alpha)^{48}Sc$ with an half-life of 43.7 hours was investigated. The experimental technique was similar to that mentioned in the previous section.

The experimental data of the present work are shown in Fig. 4 and compared with the ENDF/B-VI evaluation and with previous experiments. Our data do not confirm the structure

* Argonne National Laboratory, Argonne, USA

of the cross section around 11 MeV as indicated by the experimental data of Paulsen et al. [7] and Lu Hanlin et al. [8]. In general, our data confirm the adequate description of this cross section by the ENDF/B-VI evaluation and are consistent with the majority of previous experiments. Especially, between 13.3 and 14.4 MeV, our data are in excellent agreement with the experiment of Ikeda et al. [6]. Above 12.5 MeV, our data tend to continuously exceed the ENDF/B-VI evaluation. The deviation varies from 2% to 4% at 14 MeV, but is within the experimental uncertainties of 3 - 4% of our data.

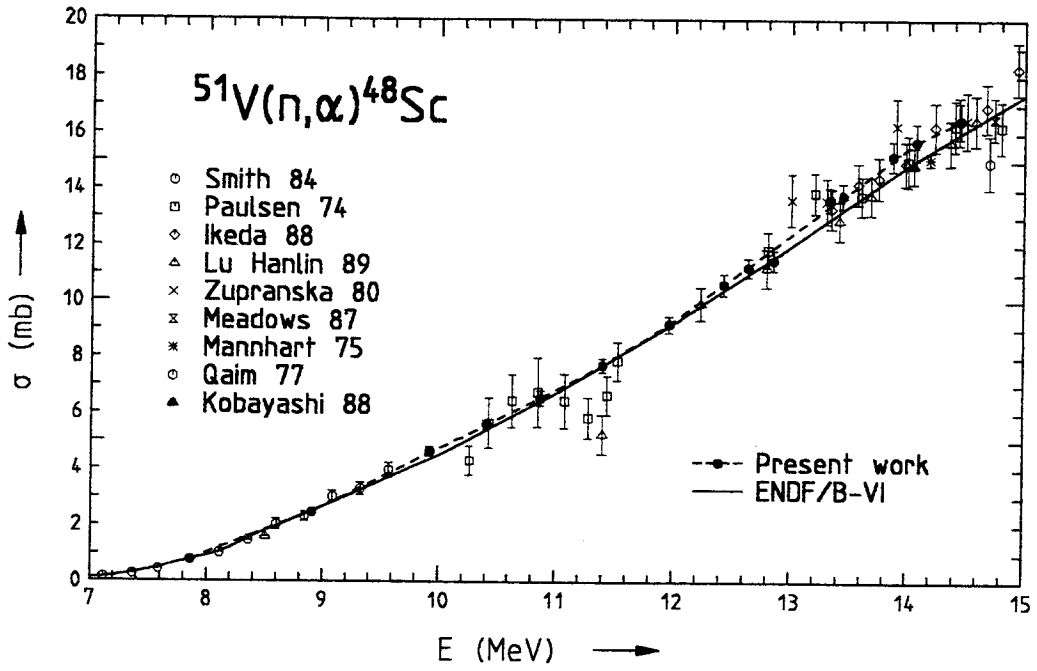

Fig. 4 Excitation function of the $^{51}V(n,\alpha)^{48}Sc$ reaction

5. Measurement of the $^{238}U(n,f)$ Cross Section at Neutron Energies of 34 MeV, 46 MeV and 61 MeV

W.D. Newhauser[+], H.J. Brede, V. Dangendorf, W. Mannhart, J.P. Meulders[*], U.J. Schrewe, H. Schuhmacher

The cross section for the neutron-induced fission in ^{238}U is one of the reference cross sections for the neutron energy region above 20 MeV [9] although only two sets of experimental data existed [10,11] which are also inconsistent. Due to these facts, this cross section was measured at energies of 34 MeV, 46 MeV and 61 MeV against the well-known n-p scattering cross section [12].

The investigations were carried out at the irradiation facility for high-energy neutrons of the Université Catholique de Louvain (UCL). The sensor for detecting the fission products was an arrangement of 10 parallel plate ionisation chambers [13] which have a detection probability of

[+] Present address: Massachusetts General Hospital, USA
[*] Université Catholique de Louvain, Louvain-la-Neuve, Belgium

96% for fission products. This chamber allows fission products to be easily distinguished from α-particles by pulse height analysis. Owing to the relatively good time resolution of about 5 ns and the time structure of the neutron beam (an external deflection system of the accelerator enabled neutron production with a time separation of 500 ns), the time-of-flight method could be used to select the above-mentioned neutron energies. The neutron fluence was determined using a recoil proton telescope.

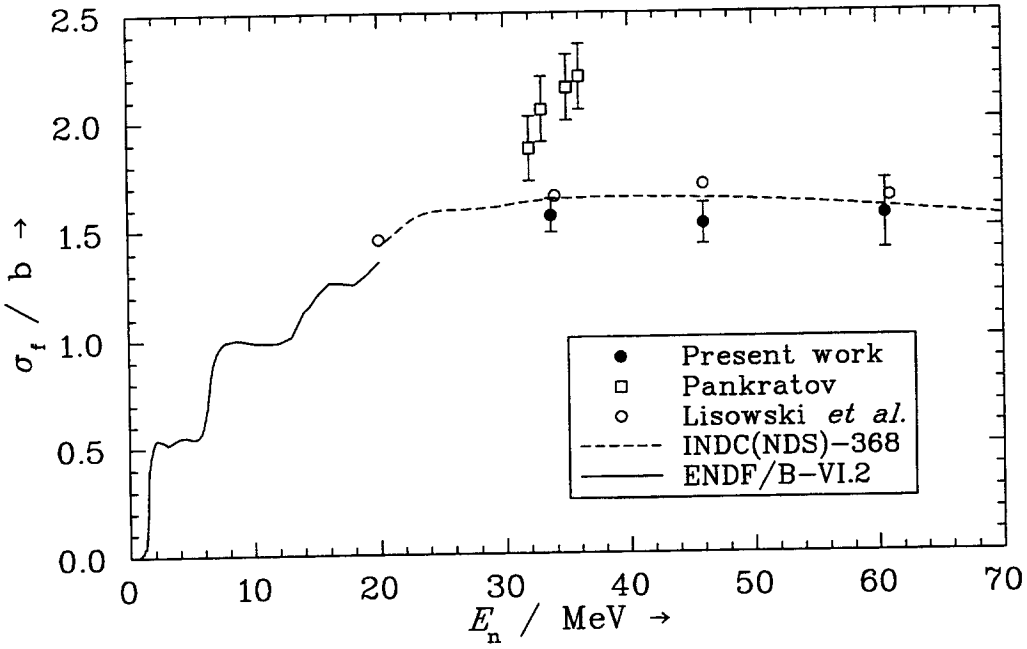

Fig. 5 Cross section for the neutron-induced fission of ^{238}U as a function of neutron energy. The results obtained are compared with those of Pankratov [10] and a selection of results of Lisowski et al. [11]. In addition, the recommended data from evaluations and are represented as lines.

In Fig. 5 the results of measurement are compared with the above-mentioned experimental data and with the recommended cross sections from evaluations. Our results confirm the data obtained by Lisowski *et al.* and show that the values of Pankratov are too high have a false energy dependence. The INDC evaluation [14] carried out recently is in agreement with our data.

References

[1] D. Schmidt, W. Mannhart, B.R.L. Siebert, Nuclear Data for Science and Technology, Conference Proceedings (G. Reffo, A. Ventura, C. Grandi, eds.), Italian Physical Society, Bologna, Vol. 59 (1997) 407

[2] D. Schmidt, W. Mannhart, B.R.L. Siebert, Progress Report (S.M. Qaim, ed.), NEA/NSC/DOC(97)13 (1997) 53, Forschungszentrum Jülich, Germany

[3] A.B. Smith, D. Schmidt, Report ANL/NDM-138 (1996), Argonne National Laboratory, Argonne, USA

[4] D. Schmidt, W. Mannhart, Report PTB-N-31 (1998), PTB Braunschweig, Germany
[5] D.L. Smith J.W. Meadows, I. Kanno, Ann. Nucl. Energy 11 (1984) 623
[6] Y. Ikeda, C. Konno, K. Oishi, T. Nakamura, H. Miyade, K. Kawade, H. Yamamoto, T. Katoh, Report JAERI-1312 (1988), JAERI, Tokai-mura, Japan
[7] A. Paulsen, R. Widera, H. Liskien, Atomkernenergie 22 (1974) 291
[8] Zhao Wengrong, Lu Hanlin, Yu Weixiang, Yuan Xialin, Report INDC(CPR)-16 (1989), IAEA, Vienna, Austria
[9] Proceedings of a Specialists' Meeting on Neutron Cross Section Standards for the Energy Region above 20 MeV, Report NEANDC-305 (1991), NEA, Paris, France
[10] V. Pankratov, Atomnaya Energiya 14 (1962) 177
[11] P. Lisowski, A. Gavron, W.E. Parker, J.L. Ullmann, S.J. Balestrini, A.D. Carlson, O.A. Wasson, N.W. Hill, Report NEANDC-305 (1991) 177, NEA, Paris, France
[12] W.D. Newhauser, H.J. Brede, V. Dangendorf, W. Mannhart, J.P. Meulders, U.J. Schrewe, H. Schuhmacher, Nuclear Data for Science and Technology, Conference Proceedings (G. Reffo, A. Ventura, C. Grandi, eds.), Italian Physical Society, Bologna, Vol. 59 (1997), 1236
[13] D. Gayther, Metrologia 27 (1990) 221
[14] A.D. Carlson, S. Chiba, F.J. Hambsch, N. Olson, A.N. Smirnov, Report INDC(NDS)-368 (1997), IAEA, Vienna, Austria

APPENDIX

Addresses of Contributing Laboratories

Institut für Kernphysik III
Director: Prof. Dr. G. Schatz
Reporter: Dr. F. Käppeler
Forschungszentrum Karlsruhe
Postfach 36 40
76021 Karlsruhe

Institut für Materialforschung I
Director: Prof. Dr. K.-H. Zum Gahr
Reporter: Dr. E. Daum
Forschungszentrum Karlsruhe
Postfach 36 40
76021 Karlsruhe

Institut für Neutronenphysik
und Reaktortechnik
Director: Prof. Dr. G. Kessler
Reporter: Dr. U. Fischer
Forschungszentrum Karlsruhe
Postfach 36 40
76021 Karlsruhe

Institut für Nuklearchemie
Director: Prof. Dr. H.H. Coenen
Reporter: Prof. Dr. S.M. Qaim
Forschungszentrum Jülich
Postfach 1913
52425 Jülich

Institut für Kern- und Teilchenphysik
Director: Prof. Dr. B. Spaan
Reporter: Prof. Dr. K. Seidel
Technische Universität Dresden
Mommsenstr. 13
01062 Dresden

Zentrum für Strahlenschutz und Radioökologie
Head: Prof. Dr. R. Michel
Reporter: DP M. Gloris
Universität Hannover
Am Kleinen Felde 30
30167 Hannover

Abteilung Nuklearchemie
Director: Prof. Dr. H.H. Coenen
Reporter: Dr. U. Herpers
Universität zu Köln
Otto-Fischer-Straße 12 - 14
50674 Köln

Institut für Kernchemie
Head and reporter: Prof. Dr. H.O. Denschlag
Universität Mainz
Fritz-Strassmann-Weg 2
55128 Mainz

Fachbereich Physikalische Chemie
Kernchemie
Reporter: Prof. Dr. P. Patzelt
Philips-Universität Marburg
Lahnberge
35043 Marburg/Lahn

FRM-II: Reaktorstation
Reporter: Dr. W. Waschkowski
Technische Universität München
85747 Garching/München

Physikalisch-Technische Bundesanstalt
Abteilung Ionisierende Strahlung
Director: Prof. Dr. G. Dietze
Reporter: Dr. W. Mannhart
Bundesallee 100
38116 Braunschweig